Turkish Journal of Earth Sciences

Volume 17 | Number 2 Article 3

1-1-2008

Petrogenesis of the Kösedağ Pluton, Suşehri-NE Sivas, East-Central Pontides, Turkey

DURMUŞ BOZTUĞ

Turkish Journal of Earth Sciences (Turkish J. Earth Sci.), **Vol. 17**, 2008, pp. 241–262. *Copyright ©TÜBİTAK*
First published online 12 December 2007

Petrogenesis of the Kösedağ Pluton, Suşehri-NE Sivas, East-Central Pontides, Turkey

DURMUŞ BOZTUĞ

Department of Geological Engineering, Cumhuriyet University, TR–58140 Sivas, Turkey
(E-mail: durmus.boztug@gmail.com)

Abstract: The Kösedağ syenite crops out as a shallow-seated pluton within the Eocene volcano-sedimentary rocks and is unconformably overlain by Lower Miocene limestones in the Suşehri-NE Sivas region, east-central Pontides. It consists of syenites and quartz syenites with a phaneritic, porphyritic texture characterized by K-feldspar megacrysts set in a coarse- to medium-grained groundmass comprising K-feldspar, plagioclase, clinopyroxene, amphibole, biotite and quartz. Major element geochemistry data reveal a high-K, alkaline, metaluminous to slightly peraluminous character, with a low Aluminum Saturation Index (ASI) value. The main solidification process, which modified the composition of magma during crystallization, was fractional crystallization, in which syenites solidified first, and quartz syenites later. Trace element geochemistry data reveal that the magma source of the Kösedağ pluton was a metasomatized mantle affected by subduction-derived fluids. This magma source could have been derived from partial melting of a metasomatized mantle layer which was accreted into the collision zone between the Eurasian plate and the Tauride-Anatolide platform along the İzmir-Ankara-Erzincan suture zone. A post-collisional extensional regime, induced by slab break-off following the continent-continent collision, may have melted these metasomatized mantle slices to produce the high-K, alkaline, metaluminous magma source of the Kösedağ syenite.

Key Words: geochemistry, geodynamics, Kösedağ pluton, central-eastern Pontides, Turkey

Kösedağ Plütonunun Petrojenezi, Suşehri-KD Sivas, İç-Doğu Pontidler, Türkiye

Özet: Kösedağ plütonu, orta Pontidlerin doğu kesiminde Suşehri-KD Sivas yöresinde Eosen yaşlı volkano-sedimanter kayaçlar içerisinde sığ sokulumlu siyenitik bir plüton olarak yüzeylenir ve Erken Miyosen (Akitaniyen) yaşlı lagünel kireçtaşları tarafından uyumsuzlukla örtülür. Kösedağ siyeniti başlıca siyenit ve kuvars siyenit bileşimli kayaçlardan oluşur. Bu kayaçlar, tipik olarak K-feldispat megakristallerinin varlığıyla belirginleşen faneritik-porfirik dokuya sahip olup; megakristaller, başlıca K-feldispat, plajiyoklaz, klinopiroksen, amfibol, biyotit ve kuvars minerallerinden oluşan kaba ve orta-taneli bir hamur içerisinde dağılmış olarak bulunurlar. Ana element jeokimyası yüksek-K'lu, alkalin, metaluminodan çok hafifçe peralüminoya değişen düşük alüminyum satürasyon indisine sahip özellikler sunmaktadır. Magmanın katılaşması sırasında fraksiyonel kristallenme süreci ile bileşimin değiştiği ve böylece siyenitlerin önce, kuvars siyenitlerin ise daha sonra oluştuğu belirlenmiştir. Eser element jeokimyası verileri, Kösedağ batoliti magmasının, daha önceki bir dalma-batma zonundan türemiş çözeltilerce metasomatizmaya uğratılmış bir metasomatik manto kaynağından türediğini gösterir. Böyle bir metasomatik kaynak malzeme, İzmir-Ankara-Erzincan kenet kuşağı boyunca Avrasya levhası ve Torid-Anatolid platformu arasında meydana gelen çarpışma zonuna tektonik dilimler olarak eklenmiş olabilir. Böyle bir manto malzemesi, kıta-kıta çarpışmasını izleyen litosferik dilim kopmasına (slab break-off) bağlı olarak meydana gelebilecek bir gerilme rejimi altında kısmi erimeye uğrayarak yüksek K'lu, alkalin, metalümino, A-tipi Kösedağ siyeniti magmasını üretmiş olabilir.

Anahtar Sözcükler: jeokimya, jeodinamik, Kösedağ plütonu, iç-doğu Pontidler, Türkiye

Introduction

The Eocene multi-sourced granitoids in the central and eastern Pontides, NE Anatolia, Turkey, crop out either as part of the composite Kaçkar batholith (Boztuğ *et al.* 2006) or as discrete intrusions in the Lower to Middle Eocene volcano-sedimentary sequence deposited in fault-controlled basins (Figure 1). Boztuğ *et al.* (2005a) reported that on the basis of differing mineralogy and geochemistry they may be subdivided into three groups: (1) An I-type, calc-alkaline, metaluminous group, consisting of the Ayder K-feldspar megacrystic granitoid (south of Çamlıhemşin-Rize; Boztuğ *et al.* 2006, 2007;

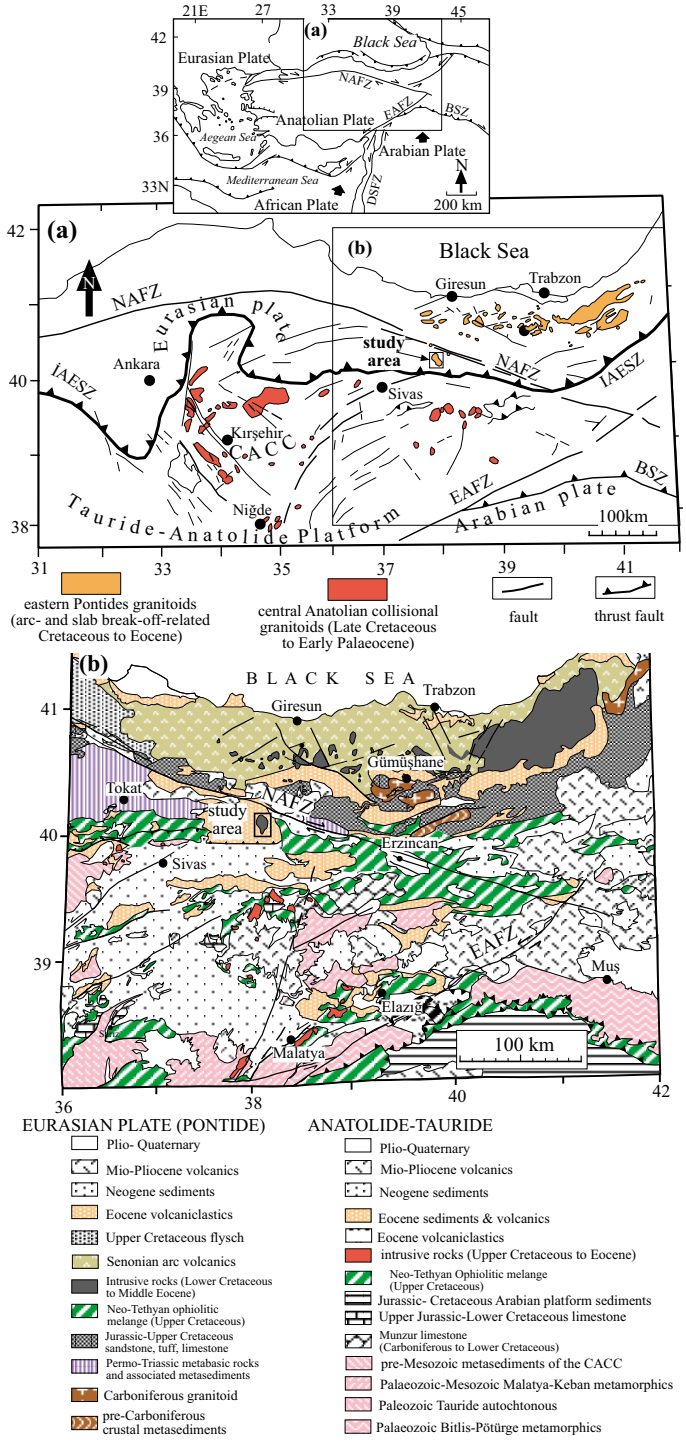

Figure 1. Location map and regional geological-geographical setting of the eastern Pontide and central Anatolian granitoids and surrounding region (simplified after Bingöl 1989; Boztuğ & Jonckheere 2007). The upper inset shows the simplified regional tectonic setting of Turkey and adjacent areas (after Bozkurt & Mittwede 2001). NAFZ– North Anatolian Fault Zone; IAESZ– İzmir-Ankara-Erzincan Suture Zone; EAFZ– East Anatolian Fault Zone; BSZ– Bitlis Suture Zone; CACC– Central Anatolian Crystalline Complex; DSFZ– Dead Sea Fault Zone.

Boztuğ & Harlavan 2007), the Uzuntarla porphyritic granodiorite (south of Araklı-Trabzon; Boztuğ & Harlavan 2007), the Dölek and Sarıçiçek granitoids (near Gümüşhane; Karslı *et al.* 2004a, b, 2007; Arslan & Aslan 2006), the Zigana granitoid (S of Maçka-Trabzon; Karslı *et al.* 2002, 2004b), and the Saraycık granitoid (near Bayburt; Topuz *et al.* 2005); (2) An A-type, alkaline, metaluminous group comprising the Çambaşı quartz syenite and Bektaşyayla quartz monzonite (SE of Ordu; Boztuğ 2001), the Kösedağ syenite (around Suşehri-Sivas; Kalkancı 1974; Boztuğ *et al.* 1994; Boztuğ 2001), the Sisdağı and Kuruçam granitoids (near Trabzon; Arslan & Aslan 2006); (3) An M-type group consisting of the medium-K, calc-alkaline to tholeiitic Halkalıtaş quartz diorite and low-K tholeiitic Ardeşen gabbro and Isina diabase, which are mainly exposed as shallow-seated small stocks and N–S-, NE–SW-, NW–SE- and E–W-trending dykes (south of Ardeşen-Rize; Boztuğ *et al.* 2006, 2007). The Rb-Sr (Kalkancı 1974), K-Ar (Taner 1977; JICA 1986; Karslı *et al.* 2004a; Boztuğ & Harlavan 2007), Ar-Ar (Topuz *et al.* 2005), U-(Th-Pb) (Delaloye *et al.* 1972), U-Pb (Arslan & Aslan 2006) and titanite fission-track ages (Boztuğ *et al.* 2007) of about 50 to 40 Ma date the emplacement and cooling of these units, and are consistent with the stratigraphic relations.

Boztuğ *et al.* (2005a) proposed that these Eocene multi-sourced granitoids could have been derived from hybrid magma sources resulting from mingling and mixing of coeval mantle- and crustal-derived melts generated in a post-collisional extension-related geodynamic setting in the east-central and eastern Pontides of NE Turkey. It has been proposed that this extensional tectonic regime resulted from slab break-off (Davies & von Blanckenburg 1995; von Blanckenburg & Davies 1995) following continent-continent collision between the Tauride-Anatolide platform (TAP) and the Eurasian plate (EP) along the İzmir-Ankara-Erzincan (IAE) suture zone (Boztuğ *et al.* 2005a).

This paper deals mainly with the geological setting, petrography and geochemistry of the Kösedağ pluton, Suşehri-NE Sivas, east-central Pontides, about which there is so far limited unpublished (Kalkancı 1974; Boztuğ 2001) and published (Boztuğ *et al.* 1994) literature data, to throw light on the genesis of the Eocene granitoid magmatism with special reference to geodynamic evolution.

Analytical Techniques

All sample preparation procedures, including thin sectioning, crushing, sieving and grinding in order to get rock powders for whole-rock geochemical analysis, were performed at the laboratories of the Department of Geological Engineering of Cumhuriyet University, Sivas, Turkey.

About 100 rock samples, collected from the Kösedağ pluton, were analysed in order to get the whole-rock major element geochemical composition. These analyses were carried out on pressed powder tablets using X-ray fluorescence spectrometry (RIGAKU 3270 E-WDS) at the Mineralogical-Petrographical and Geochemical Research Laboratories (MIPJAL) of the Department of Geological Engineering, Cumhuriyet University (Sivas) using USGS and CRPG rock standards for calibration. Analytical results from USGS, CRPG and GIT-IWG standards obtained by MIPJAL and their recommended values by Govindaraju (1989) are given in Table 1. Apart from these major element geochemical analyses, fifteen representative rock samples were chosen for trace and rare earth elements (REE) analysis, undertaken by ACTLABS in Ancaster, Ontario, Canada. Trace and REE analyses were carried out by a lithium metaborate/tetraborate fusion ICP/MS package Code 4B2-STD (for the details of analytical technique, please see: www.actlabs.com). During the trace and REE analyses, 10 international rock and mineral standards were also analysed for quality assurance (Table 2).

Four zircon grains, extracted from quartz syenite sample BAL-87, were analysed using the single zircon $^{207}Pb/^{206}Pb$ evaporation age method in order to determine the intrusion age of the Kösedağ pluton at the Mineralogical Institute of the TU Bergakademie Freiberg using a FINNIGAN MAT 262 mass spectrometer, according to the method of Kober (1986, 1987) with common lead correction of Stacey & Kramers (1975).

Regional Tectonic Setting

The Kösedağ pluton crops out at the periphery of the collision zone between the Eurasian plate (EP) (i.e. Pontides) and Tauride-Anatolide platform (TAP), north of the İzmir-Ankara-Erzincan (IAE) suture zone, NE of Sivas, east-central Pontides (Figure 1). The oldest basement rocks consist of pre-Early Jurassic Pınarlar

Table 1. Comparison of the whole-rock major element geochemical analyses results (wt%) of the GIT-IWG, CRPG and USGS rock standards by Sivas-MIPJAL and their recommended values by Govindaraju (1989).

Standards	*GIT-IWG*	MIPJAL	*CRPG*	MIPJAL	*CRPG*	MIPJAL	*CRPG*	MIPJAL	*USGS*	MIPJAL	*USGS*	MIPJAL
	AC-E	AC-E	GA	GA	GH	GH	BR	BR	SCo-1	SCo-1	AGV-1	AGV-1
SiO_2	70.35	68.18	69.90	69.71	75.80	76.08	38.20	38.33	62.78	63.72	58.79	58.59
TiO_2	0.11	0.09	0.38	0.36	0.08	0.06	2.60	2.49	0.63	0.68	1.05	1.08
Al_2O_3	14.70	14.42	14.50	15.33	12.50	11.33	10.20	9.90	13.67	14.43	17.14	16.12
tFe_2O_3	2.53	2.83	2.83	2.45	1.34	1.32	12.88	10.13	5.14	5.78	6.76	6.45
MnO	0.06	0.06	0.09	0.09	0.05	0.05	0.20	0.17	0.05	0.06	0.09	0.10
MgO	0.03	0.51	0.95	1.41	0.03	0.60	13.28	13.20	2.72	3.20	1.53	1.42
CaO	0.34	0.44	2.45	2.36	0.69	0.82	13.80	14.23	2.62	3.26	4.94	4.75
Na_2O	6.54	6.56	3.55	3.53	3.85	3.17	3.05	3.19	0.90	0.63	4.26	3.78
K_2O	4.49	4.42	4.03	4.23	4.76	4.45	1.40	1.62	2.77	2.98	2.91	2.89
P_2O_5	0.01	0.02	0.12	0.15	0.01	0.02	1.04	1.44	0.21	0.20	0.49	0.48
LOI	0.37	0.51	1.00	0.87	0.70	0.81	3.00	3.17	6.66	6.10	1.20	1.42
Total	99.53	98.04	99.80	100.49	99.81	98.71	99.65	97.87	98.15	101.04	99.16	97.08

tFe_2O_3, total iron oxide as ferric iron; LOI, loss on ignition

metamorphics in the Dereli-Giresun region of the east-central Pontides (Boztuğ *et al.* 2004), the Hercynian (Late Carboniferous) Pulur metamorphic massif (Topuz *et al.* 2004a, b, c) and the Gümüşhane granitoid in the eastern Pontides. These are unconformably overlain by Jurassic to Upper Cretaceous sedimentary and volcano-sedimentary rocks (Figure 1). A Neo-Tethyan ophiolitic mélange is unconformably covered by the Turonian Ardıçlı formation (Boztuğ *et al.* 2006) which indicates a pre-Turonian, most probably Cenomanian, ophiolite obduction in the east-central Pontide region.

Senonian arc-related volcano-sedimentary rocks and granitoid intrusions (Figure 1) constitute the well-preserved palaeo-arc environment resulting from northward subduction of the IAE ocean beneath the EP (e.g., Manetti *et al.* 1983; Akıncı 1985; Okay & Şahintürk 1997; Yılmaz *et al.* 1997; Boztuğ *et al.* 2003, 2006, 2007; Kaygusuz *et al.* 2007). Boztuğ *et al.* (2006, 2007) reported the existence of Early to Late Cretaceous arc-related and Paleocene to Middle Eocene syn- to post-collisional granitoids in the composite Kaçkar batholith between Ardeşen (Rize) in the north and İspir (Erzurum) in the south (Figure 1).

The final collision between TAP and EP is thought to have occurred in the Late Palaeocene–Early Eocene, based on structural (Şengör & Yılmaz 1981; Okay & Şahintürk 1997; Yılmaz *et al.* 1997) and apatite fission-track data (Boztuğ *et al.* 2004). Therefore, the Eocene volcano-sedimentary sequence, deposited mostly in E–W- and NE–SW-oriented basins, marks the start of a new volcanic and sedimentary cycle resulting from a regional extensional regime (Okay & Şahintürk 1997; Yılmaz *et al.* 1997), which also accelerated the opening of the Eastern Black Sea Basin (Okay *et al.* 1994; Okay & Şahintürk, 1997; Kazmin *et al.* 2000). Most recently, Boztuğ *et al.* (2005a, 2007) and Boztuğ & Harlavan (2007) proposed that this regional extension resulted from slab break-off following the Late Palaeocene–Early Eocene continent-continent collision between the TAP and EP in the east-central and eastern Pontides.

Oligocene to Late Miocene evolution of the eastern Pontides is reportedly characterized by shortening resulting from the convergence between Eurasia and Africa-Arabia (e.g., Okay & Şahintürk 1997). Hubert-Ferrari *et al.* (2002) proposed that most of this convergence was accommodated by south-verging thrusts and folds along the southeast-verging İzmir-Ankara-Erzincan suture. More recently, apatite fission-track geothermochronology studies carried out in the Kösedağ pluton (Boztuğ & Jonckheere 2007) and composite

Table 2. Comparison of the whole-rock trace and REE geochemical analyses results (ppm) of 10 different international rock and mineral standards by Actlabs, Ancaster, Canada (A) and their certified (C) values.

Element	MAG1		BIR1		DNC1		GXR2		LKSD3		MICA Fe		GXR1		SY3		STM1		IFG1	
	A	C	A	C	A	C	A	C	A	C	A	C	A	C	A	C	A	C	A	C
V	132	140	313	313	161	148	47	52	76	82	152	135	89	80	49	50	-5	8.7	11	2
Cr	100	97	385	382	270	285	35	36	85	87	97	90	-40	12	-40	11	-20	4.3	-20	4
Co	21	20.4	51	51.4	54	54.7	8	8.6	31	30	27	23	8	8.2	8	8.8	-1	0.9	31	29
Ni	52	53	170	166	248	247	-20	21	55	47	38	35	44	41	-40	11	-20	3	30	23
Cu	29	30	131	126	98	96	71	76	35	35	-10	5	1110	1110	25	17	-10	4.6	12	13
Zn	129	130	74	71	61	66	133	530	-30	152	1140	1300	763	760	248	244	233	235	-30	20
Ga	22	20.4	16	16	14	15	37	37	15	nd	97	95	17	14	31	27	37	36	-1	0.7
As	10	9.2	-5	0.4	-5	0.2	39	25	46	27	-5	3	427	427	26	19	-5	4.6	-5	1.5
Rb	149	149	-2	0.25	4	4.5	76	78	77	78	2150	2200	-4	14	207	206	120	118	-2	4
Sr	138	146	10	108	140	145	152	160	246	240	4	5	290	275	298	302	697	700	4	3
Y	27	28	16	16	18	18	18	17	30	30	46	48	31	32	791	718	46	46	11	9
Zr	114	126	15	16	33	41	228	269	152	178	808	800	27	38	324	320	1210	1210	-5	1
Nb	14	12	-1	0.6	1	3	10	11	8	8	274	270	-2	0.8	123	148	264	268	-1	0.1
Mo	-2	1.6	-2	0.5	-2	0.7	2	2.1	-2	<5	-2	1.2	17	18	-4	1	6	5.2	-2	0.7
Sn	3	3.6	-1	0.65	1	nd	2	1.7	2	3	70	70	53	54	9	6.5	12	6.8	3	0.3
Sb	0.7	0.96	0.6	0.58	0.8	0.96	37.6	49	1.3	1.3	-0.5	nd	75	122	-1	0.31	1.7	1.66	0.7	0.63
Cs	8.6	8.6	-0.5	0.005	-0.5	0.34	5.1	5.2	2.3	2.3	171	180	3	3	3	3	1.6	1.54	-0.5	0.06
Ba	486	479	7	7	100	114	2240	2240	654	680	143	150	914	750	435	450	596	560	9	1.5
La	41.9	43	1.4	0.62	4	3.8	25.4	25.6	50	52	198	200	9	7.5	1170	1340	154	150	4	2.8
Ce	86.1	88	2.4	1.95	8.5	10.6	51.1	51.4	93.2	90	416	420	15.5	17	1950	2230	266	259	4.8	4
Pr	10.06	9.3	0.51	0.38	1.14	1.2	5.51	nd	12	nd	50.9	49	2.1	nd	222	223	26.4	19	0.6	0.4
Nd	36.2	38	2.5	2.5	4.9	4.9	19.6	19	43.1	44	176	180	8.6	18	716	670	80.2	79	2.2	0.2
Sm	7	7.5	1.1	1.1	1.4	1.38	3.6	3.5	7.9	8	33.2	33	2.9	2.7	127	109	12.4	12.6	0.5	0.4
Eu	1.46	1.55	0.54	0.54	0.61	0.59	0.79	0.81	1.49	1.50	0.63	0.7	0.6	0.69	19.2	17	3.66	3.6	0.42	0.39
Gd	6.1	5.8	1.9	1.85	2.1	2	3.1	3.3	6.4	nd	22.1	21	4.1	4.2	129	105	9.3	9.5	0.8	0.74
Tb	1	0.96	0.4	0.36	0.4	0.41	0.5	0.48	1	1	2.7	2.7	0.8	0.83	23.5	18	1.6	1.55	0.1	0.11
Dy	5	5.2	2.6	2.5	2.7	2.7	2.8	3.3	5	4.9	10.3	11	4.7	4.3	136	118	8.1	8.1	0.9	0.8
Ho	1	1.02	0.6	0.57	0.6	0.62	0.6	nd	1	nd	1.4	1.6	0.9	nd	29.6	29.5	1.5	1.9	0.2	0.2
Er	2.9	3	1.8	1.7	2	2	1.8	nd	3.1	nd	3.8	3.8	2.8	nd	93.6	68	4.7	4.2	0.7	0.63
Tm	0.43	0.43	0.28	0.26	0.32	0.33	0.29	0.3	0.45	nd	0.55	0.8	0.4	0.43	13.9	11.6	0.7	0.69	0.11	0.09
Yb	2.6	2.6	1.7	1.65	2	2.01	1.8	2.04	2.9	2.7	3.4	3.5	2.3	1.9	72.2	62	4.6	4.4	0.6	0.6
Lu	0.39	0.40	0.26	0.26	0.31	0.32	0.29	0.27	0.44	0.4	0.49	0.5	0.32	0.3	8.96	7.9	0.67	0.6	0.1	0.09
Hf	3.5	3.7	0.6	0.6	1	1.01	6.5	8.3	4.5	4.8	26.2	26	0.8	1	9.9	9.7	27.9	28	-0.2	0.04
Ta	1.2	1.1	-0.1	0.04	-0.1	0.098	0.8	0.9	0.6	0.7	32.7	35	-0.2	0.175	14.4	30	19.6	18.6	0.2	0.2
W	1	1.4	-1	0.07	-1	0.2	2	1.9	-1	<4	8	15	150	164	9	1.1	4	3.6	223	220
Tl	0.3	0.59	-0.1	0.1	-0.1	0.026	0.5	1.03	0.3	nd	16	16	0.5	0.39	1.7	1.5	0.3	0.26	-0.1	0.02
Pb	21	24	-5	3	7	6.3	112	690	-5	29	7	13	730	730	93	133	21	17.7	-5	4
Bi	-0.4	0.34	-0.4	0.02	-0.4	0.02	-0.4	0.69	-0.4	nd	-0.4	2	1380	1380	3.6	0.8	2.1	0.13	-0.4	nd
Th	11	11.9	-0.1	0.03	0.2	0.2	7.9	8.8	10.2	11.4	151	150	2.4	2.44	778	1003	29.4	31	-0.1	0.1
U	2.9	2.7	-0.1	0.01	-0.1	0.1	3	2.9	4.7	4.6	90.2	80	34.2	34.9	560	650	9.6	9.06	-0.1	0.02

Negative values = not detected at that lower limit; nd, not determined.

Kaçkar batholith between Ardeşen (Rize) and Ispir (Erzurum) (Boztuğ *et al.* 2005b) yielded an Oligocene (28–29 Ma) and an Early Miocene (20 Ma) accelerated uplift, respectively. Boztuğ & Jonckheere (2007) and Boztuğ *et al.* (2005b) interpreted both of these accelerated uplift events to be connected with the closure of the Bitlis ocean and the collision of the African-Arabian and Eurasian plates along the Bitlis-Zagros suture zone, on the basis of considerations given by Şengör *et al.* (2003). The continued convergence initiated the dextral North Anatolian Fault Zone, setting off the westward escape of the Anatolian block (Şengör & Kidd 1979; Bozkurt 2001; Bozkurt & Mittwede 2001) from the Late Miocene (Şengör *et al.* 1985; Hempton 1987; Le Pichon *et al.* 1988) through the Early Pliocene (Barka 1992; Westaway 1994) to the Late Pliocene (Şaroğlu 1988; Trifonov *et al.* 1994).

Geological Setting

The Kösedağ pluton intrudes the Aksu formation consisting of volcano-sedimentary rocks in which the limestone lenses yield Eocene fossils (Kalkancı 1974), and unconformably covered by the Early Miocene Yukarıakören limestone. Fossils, found in the Yukarıakören limestone include *Austrotrillina howchini (Schlumberger), Archaias kirkukensis Henson, Peneroplis sp., Dendritina sp., Miliolidae, Gastropoda, Echinoidae,* which indicate an Early Miocene (Aquitanian) lagoonal environment (Boztuğ 2001) (Figure 2). The syenitic rocks can be subdivided into syenites and quartz syenites, on the basis of quartz content. The syenitic rocks were mainly observed in the northern and southern parts, whereas the quartz syenites are exposed in the central part of the present outcrop (Figure 2). The only finer-grained microsyenites crop out between Kemikçukuru yayla in the west and Aşağıören yayla in the east, and trend roughly N–S (Figure 2). The Yukarıakören limestone also overlies these microsyenites unconformably at high altitudes in this location (Figure 2). No mappable and significant contact metamorphic aureole surrounds the Kösedağ pluton, although it seems to be a shallow-seated granitoid intrusion. The limited contact metamorphic rocks consist mainly of albite-epidote-tremolite/actinolite hornfelses derived from the basic to intermediate volcanics of the Aksu formation. However, there are widespread hydrothermal alteration zones characterized by white-grey kaolinitization and sericitization, greenish epidotization, chloritization and brownish-red iron oxide occurrences. These hydrothermal alteration zones were developed both within the Kösedağ pluton itself and the Aksu formation and are called the Gemindere and Maden metasomatic units, respectively (Figure 2). The main faults in the mapped area comprise a NE–SW-trending fault set with unknown motion along the fault planes which are marked by crushed and mylonitizated rocks and deep valleys in the field. These faults are considered to postdate the Early Miocene since they cut the Yukarıakören limestone (Figure 2). Two young basaltic outcrops trending N–S within the central part of the Kösedağ syenite outcrop have been described as the Tüylüdere volcanics of Pliocene age (?) in the light of regional correlation by Boztuğ (2001) (Figure 2).

Rock Description

Microscope studies show that the Kösedağ pluton consists mainly of syenitic and quartz syenitic rocks with a phaneritic-porphyritic texture characterized by the existence of K-feldspar megacrysts set in a coarse- to medium-grained groundmass composed essentially of K-feldspar, plagioclase (An_{32-48}), clinopyroxene (augite, diopsitic augite and aegirine-augite), amphibole (tremolite/actinolite and scarce primary hornblende), reddish-brown biotite and quartz. Accessory minerals include apatite, titanite and zircon. Most of the K-feldspar crystals in the groundmass typically contain plagioclase and clinopyroxene inclusions of small-tabular or stubby-prismatic habits. Secondary minerals mainly include sericite, epidote, chlorite and opaque minerals found especially within biotite.

Rock nomenclature was carried out using the mineralogical-chemical classification of Debon & Le Fort (1983). The analysed rock samples essentially plot in the syenite and quartz syenite fields, with few spreading into the monzonite and quartz monzonite subfields (Figure 3). This is very consistent with the mineralogical composition, in which quartz syenites typically have more quartz, perthitic K-feldspar and possess micrographic textures compared to the syenites. On the other hand, samples plotting in the quartz monzonite and monzonite subfields, are very similar to syenites with respect to their textural feature and mineralogical composition.

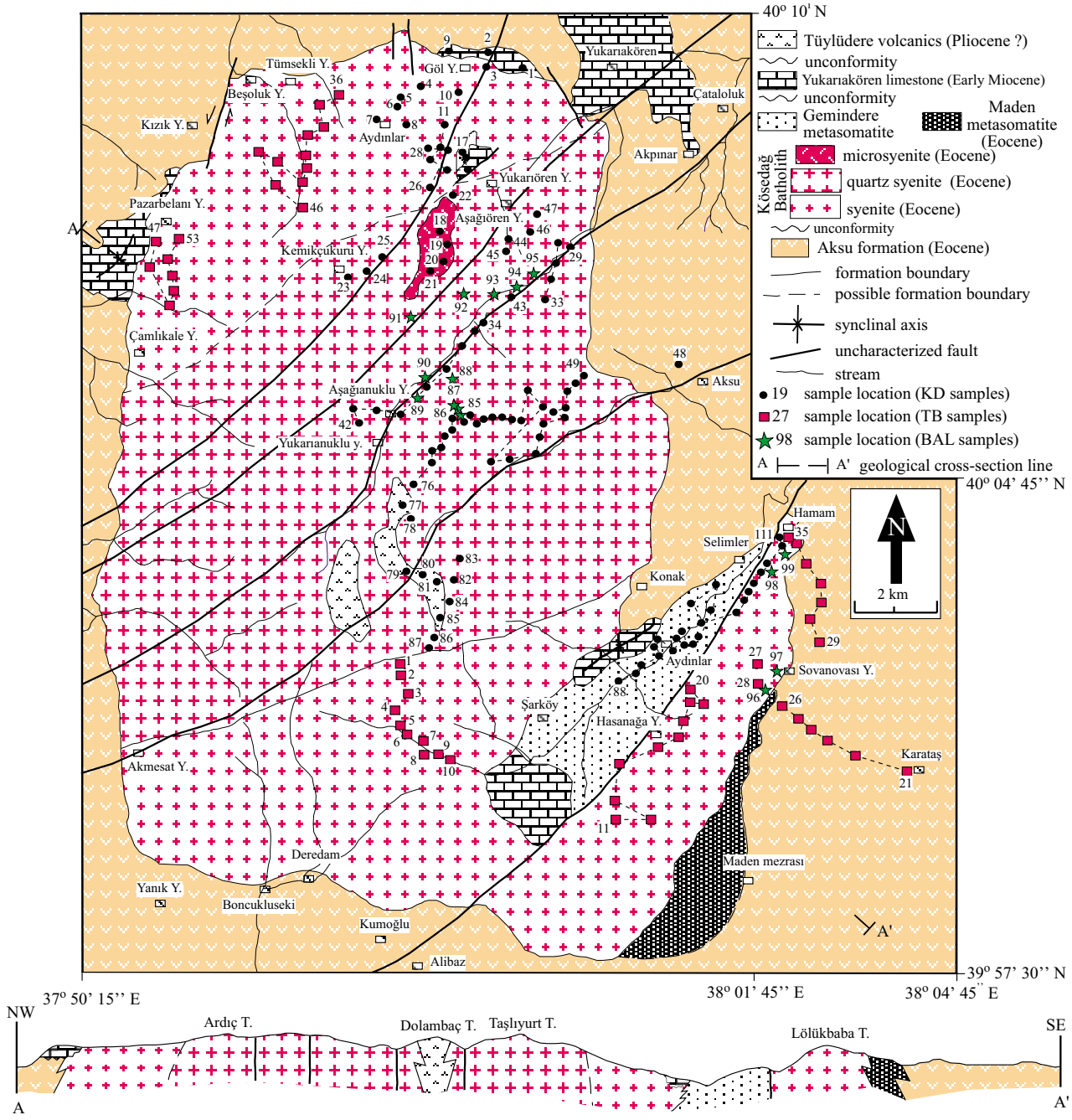

Figure 2. Geological map of the Kösedağ syenitic pluton, Suşehri-NE Sivas region, east-central Pontides, Turkey (after Boztuğ 2001) (see Figure 1 for location).

Geochemistry

Major element geochemical compositions (Table 3) of fresh samples from the Kösedağ syenitic pluton are typically alkaline (Figure 4a), high-K (Figure 4b) and metaluminous (Figure 4c), although some highly-evolved quartz syenites have a peraluminous composition due presumably to fractional crystallization (FC) (Figure 4c). The ASI (Aluminum Saturation Index= molar Al_2O_3/molar ($CaO+Na_2O+K_2O$); White & Chappell 1988) value of the Kösedağ rock samples ranges from 0.83 to 1.08 (Table

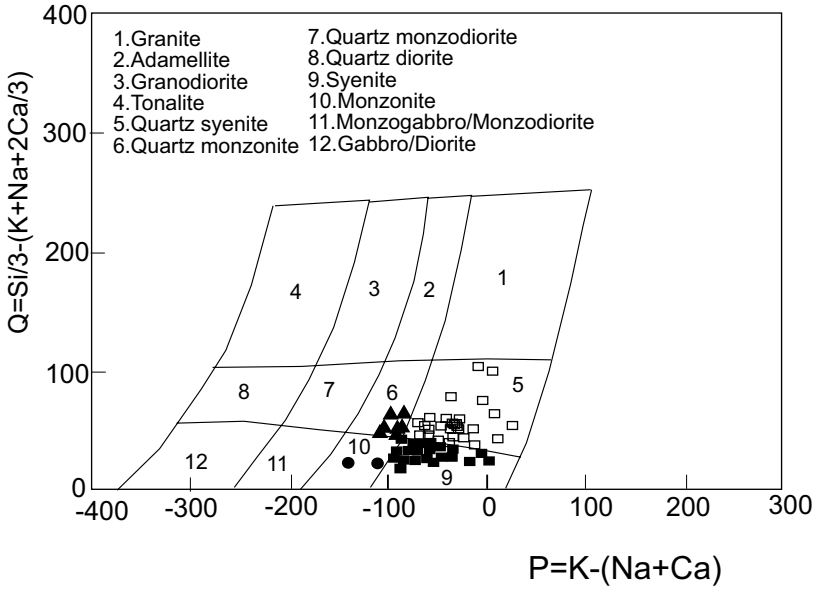

Figure 3. QP plot (Debon & Le Fort 1983) for samples from the Kösedağ syenitic pluton.

3, Figure 4d) which seems to be associated mainly with I-type granites (Chappell & White 1974), although Clarke (1992, p.9) reported that the ASI value of A-type granites can attain up to 1.075. When the ASI values of the Kösedağ rock samples are combined with their alkaline trend on a total alkalis – silica plot (Figure 4a), they emerge as having an A-type composition with a low ASI value. However, such a low ASI parameter is consistent with the mafic mineral assemblage consisting of clinopyroxene+amphibole+biotite (Chappell & White 1974; White & Chappell 1988).

Major element versus silica variation diagrams support a FC trend from monzonites through syenites to quartz syenites. Al_2O_3, tFe_2O_3, MgO, CaO, TiO_2, MnO and P_2O_5 contents decrease with increasing silica content (Figure 5a–g), and, conversely, the alkalis show a positive correlation with silica content (Figure 5h, i) with the exception of three quartz syenites samples whose silica contents are very high (close to ca. 70%), albeit with medium-level Na_2O contents (Figure 5h).

In a chondrite-normalized (normalizing values taken after Sun & McDonough 1989) REE spider diagram, the syenite and quartz syenite samples from the Kösedağ pluton have concave-upward profiles (Figure 6). Eu anomalies mark the only difference between them. Syenites have no significant Eu anomaly, with a Eu/Eu* [= $Eu_{CN}/(Sm_{CN}$ X $Gd_{CN})^{0.5}$] ranging from 0.95 through 1.14 to 1.55, except for sample BAL-96 with Eu/Eu*= 0.40 (4 samples; Table 4), but the quartz syenites have a characteristic negative Eu anomaly with Eu/Eu* ranges from 0.30 to 0.92 (11 samples, Table 4) (Figure 6). Neither syenites, nor quartz syenites reveal much fractionation between LREE and HREE and $(La/Yb)_{CN}$ ratios are generally low (6.38 to 9.78) (Table 4, Figure 6). Primitive mantle-normalized (normalizing values taken after Sun & McDonough 1989) trace element spider diagrams of the syenites and quartz syenites are very similar with negative anomalies of Ba, Nb, Sr and positive anomalies of Th, U, Pb (Figure 6). However, the quartz syenites have slightly elevated contents of Th, U, Ta, La, Zr, Hf and decreased Eu relative to the syenites (Figure 6).

Single Zircon ^{207}Pb-^{206}Pb Evaporation Age

The analysed zircon grains yield a single zircon $^{207}Pb/^{206}Pb$ evaporation age with a weighted mean age (WMA) of 52.1±6.4 Ma (MSWD = 0.90) (Table 5; Figure 7). This age agrees with the error range of the Rb-Sr whole-rock isochron age for the Kösedağ pluton (42±4 Ma) determined by Kalkancı (1974). However, a reliable single zircon ^{207}Pb-^{206}Pb evaporation age determination should have two basic fundamentals which are (1) the

Table 3. Whole-rock major element composition (wt%) of the Kösedağ syenitic pluton.

Sample	KD3/2	KD4/2	KD5	KD6	KD8/1	KD8/2	KD10	KD11	KD12	KD13	KD16	KD17
Rock type	qsy	qmz	sy	sy	sy	qsy	sy	sy	sy	sy	sy	sy
SiO_2	67.38	61.42	59.77	59.18	60.50	59.32	60.02	60.74	61.43	59.25	64.01	63.49
Al_2O_3	16.48	16.78	17.07	17.04	17.52	16.57	17.72	17.51	17.61	17.03	17.26	16.53
TiO_2	0.28	0.61	0.62	0.65	0.66	0.59	0.67	0.56	0.63	0.60	0.54	0.48
tFe_2O_3	2.21	5.86	5.87	5.41	5.35	4.92	5.69	3.76	4.72	4.18	4.47	4.01
MnO	0.06	0.12	0.11	0.14	0.15	0.13	0.13	0.10	0.12	0.08	0.16	0.10
MgO	0.20	2.45	2.69	2.56	1.87	2.27	2.24	1.57	1.77	1.91	0.55	0.77
CaO	1.10	3.80	3.22	3.42	3.20	3.38	3.48	2.50	3.11	3.10	1.95	2.21
Na_2O	4.21	4.03	4.29	4.09	4.22	3.82	4.23	4.15	4.26	4.15	5.75	5.38
K_2O	7.11	4.77	5.53	5.45	5.78	5.78	5.52	6.82	6.15	6.02	6.13	5.85
P_2O_5	0.07	0.24	0.28	0.29	0.30	0.27	0.29	0.24	0.26	0.29	0.18	0.20
LOI	0.37	1.03	0.90	0.74	0.16	1.05	0.82	0.08	1.09	1.47	0.43	0.07
ASI	0.99	0.89	0.90	0.90	0.92	0.88	0.92	0.93	0.91	0.89	0.87	0.85
Total	99.47	101.11	100.35	98.97	99.71	98.15	100.81	98.03	101.15	98.08	101.43	99.09

Sample	KD18	KD19	KD20	KD22	KD23	KD24	KD25	KD28	KD32	KD34	KD35	KD36
Rock type	sy	qsy	qsy	qsy	qsy	qmz	sy	sy	sy	qsy	qsy	sy
SiO_2	65.25	65.39	64.39	61.22	62.58	60.36	59.74	61.07	59.50	63.80	59.98	59.52
Al_2O_3	17.17	17.26	17.10	17.92	16.73	16.99	17.68	17.92	16.64	17.41	16.96	17.04
TiO_2	0.52	0.55	0.48	0.66	0.50	0.70	0.71	0.57	0.58	0.62	0.63	0.66
tFe_2O_3	3.58	4.14	3.46	4.99	4.40	6.21	5.79	4.38	4.49	4.61	4.70	4.86
MnO	0.09	0.06	0.09	0.15	0.14	0.14	0.14	0.11	0.09	0.08	0.13	0.11
MgO	0.50	0.60	0.53	1.15	1.81	2.83	2.19	1.61	2.63	1.16	2.04	2.05
CaO	1.35	2.02	1.80	2.72	2.46	3.78	3.32	3.02	3.34	2.02	2.91	3.05
Na_2O	5.27	4.38	4.93	4.31	4.20	3.99	4.22	4.29	3.83	4.26	4.14	3.91
K_2O	6.78	6.57	6.13	6.64	5.76	5.10	5.99	6.25	5.99	6.33	5.74	6.24
P_2O_5	0.12	0.19	0.18	0.27	0.21	0.31	0.32	0.26	0.28	0.21	0.30	0.31
LOI	0.82	0.53	0.04	0.23	0.54	0.59	0.68	1.16	0.78	0.56	0.53	0.29
ASI	0.92	0.95	0.94	0.92	0.94	0.89	0.90	0.92	0.88	0.99	0.92	0.90
Total	101.45	101.87	99.13	100.26	99.33	101.00	100.78	100.64	98.15	101.06	98.06	98.04

Sample	KD37	KD38	KD39	KD40	KD41	KD43	KD44	KD45	KD46	KD49	KD51	KD52
Rock type	qsy	sy	qsy	qsy	qsy	qsy	sy	mz	sy	qsy	sy	qsy
SiO_2	58.77	61.08	62.39	64.15	70.26	61.73	58.81	57.64	58.66	64.11	63.78	63.98
Al_2O_3	17.11	17.84	16.73	16.52	16.64	16.44	17.95	16.85	16.62	18.02	17.36	17.29
TiO_2	0.70	0.63	0.50	0.43	0.32	0.55	0.62	0.73	0.62	0.70	0.56	0.53
tFe_2O_3	5.33	4.58	3.32	3.00	2.28	4.21	5.65	6.19	4.85	4.56	3.64	3.34
MnO	0.12	0.11	0.06	0.09	0.04	0.12	0.12	0.11	0.11	0.15	0.11	0.12
MgO	3.16	1.45	2.36	1.06	0.13	1.87	2.42	2.85	2.82	nd	0.41	0.05
CaO	2.68	3.07	1.99	1.88	0.65	2.40	3.95	3.92	2.92	0.89	2.09	1.11
Na_2O	4.12	4.65	4.23	4.38	4.26	4.00	4.18	3.90	3.77	3.74	4.66	4.18
K_2O	5.33	5.96	6.26	6.30	6.64	6.23	5.47	5.02	6.25	8.57	7.14	7.81
P_2O_5	0.30	0.27	0.20	0.17	0.06	0.22	0.31	0.36	0.28	0.19	0.17	0.18
LOI	0.65	1.35	0.69	0.28	0.38	0.54	0.76	1.20	1.13	1.03	1.52	0.70
ASI	0.98	0.90	0.96	0.94	1.08	0.92	0.89	0.88	0.90	1.05	0.90	0.99
Total	98.25	100.99	98.73	98.26	101.66	98.26	100.24	98.77	98.03	101.96	101.44	99.29

Table 3. (Continued)

Sample	KD53	KD56	KD57	KD58	KD59	KD60	KD61	KD62	KD64	KD65	KD66	KD67	KD68
Rock type	qsy	mz	sy	qsy	qsy	qsy	qsy	sy	qsy	qsy	qsy	qsy	qsy
SiO_2	66.95	55.50	63.95	62.90	64.32	65.33	66.77	64.90	65.74	67.11	66.86	67.23	64.59
Al_2O_3	16.66	17.89	17.39	17.55	17.87	17.22	17.03	18.26	17.29	17.39	17.29	17.26	17.45
TiO_2	0.60	0.73	0.53	0.62	0.52	0.46	0.43	0.54	0.48	0.53	0.53	0.51	0.53
tFe_2O_3	3.42	6.47	3.51	4.48	3.50	2.58	3.31	3.31	2.95	3.05	3.04	2.63	2.93
MnO	0.11	0.13	0.10	0.11	0.08	0.10	0.01	0.09	0.09	0.09	0.08	0.08	0.09
MgO	nd	2.66	0.84	1.43	0.83	0.40	0.84	0.38	0.29	0.44	0.12	0.15	0.23
CaO	0.70	5.77	2.12	2.50	1.79	1.33	1.64	1.65	1.33	1.33	1.04	1.07	1.11
Na_2O	4.21	3.93	4.68	4.48	4.66	4.50	4.38	4.74	4.84	4.94	4.93	5.02	4.69
K_2O	8.18	4.20	6.49	5.98	6.83	7.15	6.21	7.72	6.70	6.79	7.03	6.82	7.41
P_2O_5	0.09	0.44	0.17	0.26	0.15	0.12	0.12	0.15	0.11	0.10	0.09	0.09	0.13
/LOI	0.74	0.83	1.27	0.82	0.49	0.42	0.98	0.20	0.59	0.14	0.20	0.47	2.02
ASI	0.97	0.83	0.90	0.95	0.97	0.98	1.00	1.00	0.98	0.97	0.98	0.98	0.98
Total	101.57	98.55	101.04	101.12	100.96	99.61	101.72	101.93	100.41	101.91	101.20	101.40	101.17

Sample	KD69	KD70	KD71	KD72	KD73	KD74	KD75	KD78	KD82	KD84	KD85	KD86	KD87
Rock type	qsy	qsy	sy	qsy	qsy	sy	qsy	qsy	sy	qsy	qmz	qsy	qsy
SiO_2	66.28	65.48	64.82	66.36	66.05	58.82	70.29	60.99	59.98	64.96	64.71	62.97	61.63
Al_2O_3	17.26	17.07	17.87	17.57	17.05	17.16	16.52	17.37	17.20	16.89	18.08	17.59	17.43
TiO_2	0.59	0.62	0.66	0.47	0.52	0.67	0.32	0.54	0.56	0.56	0.43	0.62	0.55
tFe_2O_3	3.23	2.97	3.43	2.85	3.42	5.42	1.98	4.46	4.47	3.88	3.45	4.67	3.97
MnO	0.12	0.11	0.14	0.09	0.09	0.14	0.03	0.09	0.11	0.10	0.10	0.10	0.08
MgO	0.37	0.38	0.30	0.54	0.57	2.40	nd	2.00	2.09	1.54	0.94	1.23	1.97
CaO	1.23	1.16	1.30	1.14	1.14	3.20	0.69	2.64	3.19	1.96	2.33	1.70	2.15
Na_2O	4.94	4.78	5.07	5.12	5.03	4.31	4.13	4.24	4.47	4.91	5.27	4.81	4.42
K_2O	7.07	7.15	7.03	6.98	6.90	5.48	7.01	5.63	5.51	5.69	5.07	6.29	5.82
P_2O_5	0.13	0.13	0.15	0.11	0.19	0.32	0.05	0.26	0.25	0.15	0.14	0.23	0.21
LOI	0.26	0.01	0.43	0.71	1.04	0.56	0.68	1.85	1.46	1.21	0.63	1.15	0.78
ASI	0.95	0.96	0.97	0.97	0.95	0.91	1.02	0.97	0.87	0.94	0.98	0.98	0.99
Total	101.48	99.86	101.20	101.94	101.95	98.48	101.70	100.07	99.29	101.65	101.08	101.36	99.01

Sample	KD88/1	KD92	KD93	KD94	KD100	KD104	KD108	KD109	KD111	TB5	TB6	TB7	TB8
Rock type	qsy	sy	sy	qsy	qsy	sy	sy	sy	sy	sy	sy	sy	qsy
SiO_2	64.61	61.37	60.29	65.52	64.78	56.61	59.90	59.35	56.81	60.17	59.22	57.00	60.75
Al_2O_3	17.27	17.27	16.56	16.82	17.20	17.75	17.34	17.58	17.43	17.48	17.68	16.76	17.89
TiO_2	0.51	0.68	0.70	0.59	0.67	0.69	0.66	0.65	0.79	0.63	0.68	0.73	0.56
tFe_2O_3	3.61	4.16	3.64	2.88	3.47	6.22	5.04	5.22	7.34	4.64	4.83	5.27	4.30
MnO	0.09	0.13	0.12	0.10	0.05	0.12	0.10	0.12	0.14	0.11	0.17	0.16	0.11
MgO	1.07	0.85	0.99	0.29	0.21	2.61	2.33	2.03	2.99	2.43	2.24	2.84	2.79
CaO	1.55	1.81	1.58	1.16	0.74	4.12	2.81	3.43	4.46	3.15	2.94	3.27	2.31
Na_2O	4.59	4.05	4.09	4.54	4.16	4.01	4.19	4.14	3.83	4.36	4.10	4.28	4.08
K_2O	6.47	7.80	7.28	7.18	7.29	5.55	6.06	6.05	5.41	5.29	5.95	5.15	5.94
P_2O_5	0.14	0.22	0.16	0.10	0.08	0.42	0.30	0.28	0.45	0.31	0.33	0.30	0.26
LOI	1.21	2.48	5.23	1.75	2.11	0.61	0.77	1.46	0.61	0.39	2.46	2.42	2.18
ASI	1.00	0.93	0.93	0.96	1.06	0.88	0.93	0.89	0.86	0.93	0.95	0.90	1.03
Total	101.13	100.82	100.64	100.96	100.77	98.73	99.51	100.33	100.28	98.96	100.60	98.18	101.1

Table 3. (Continued)

Sample	TB9	TB10	TB11	TB12	TB13	TB15	TB16	TB17	TB19	TB27	TB34	TB38	TB39
Rock type	qsy	qsy	qsy	mz	qsy	sy	sy	sy	qsy	sy	mz	sy	sy
SiO_2	62.20	62.03	66.11	59.96	63.63	60.26	60.02	60.57	62.45	63.62	58.67	60.64	57.09
Al_2O_3	17.54	17.21	16.98	17.64	17.31	17.17	17.46	18.32	16.97	17.85	18.55	18.24	16.70
TiO_2	0.46	0.58	0.49	0.56	0.46	0.57	0.61	0.44	0.56	0.44	0.71	0.62	0.65
tFe_2O_3	3.58	4.11	2.92	4.43	2.73	3.90	4.48	2.89	3.12	2.52	6.07	4.52	4.70
MnO	0.14	0.11	0.09	0.11	0.07	0.12	0.10	0.07	0.09	0.07	0.12	0.11	0.10
MgO	1.89	2.14	0.91	2.35	1.17	2.17	2.41	1.23	1.30	1.02	2.36	2.15	2.58
CaO	2.26	2.51	0.93	3.19	1.38	2.30	2.84	2.78	1.64	1.63	4.11	3.35	3.46
Na_2O	4.52	4.36	4.77	4.55	4.66	4.33	4.55	4.43	4.49	4.85	4.53	4.51	3.86
K_2O	5.63	5.66	6.68	5.23	6.69	6.15	5.96	6.46	6.79	6.85	5.09	5.57	5.30
P_2O_5	0.22	0.27	0.12	0.33	0.16	0.26	0.30	0.22	0.20	0.19	0.43	0.30	0.35
LOI	1.50	0.77	0.45	0.50	0.48	0.84	1.23	1.31	0.87	0.20	0.71	1.10	4.01
ASI	0.99	0.96	1.01	0.93	0.99	0.95	0.91	0.94	0.95	0.97	0.90	0.97	0.91
Total	99.94	99.75	100.45	98.85	98.74	98.07	99.95	98.72	98.48	99.24	101.35	101.11	98.80

Sample	TB40	TB41	TB42	TB43	TB44	TB45	TB46	TB48	TB49	TB50	TB51	TB52	TB53
Rock type	qmz	sy	qmz	qsy	qmz	sy	qmz	sy	sy	sy	sy	sy	sy
SiO_2	58.09	57.40	60.51	59.87	62.27	57.74	59.90	60.12	56.47	59.36	60.12	59.99	59.04
Al_2O_3	16.50	16.53	17.07	17.56	17.15	16.86	17.68	18.09	16.17	17.68	17.88	17.40	17.81
TiO_2	0.62	0.56	0.56	0.73	0.58	0.64	0.62	0.65	0.53	0.71	0.67	0.55	0.57
tFe_2O_3	5.04	4.42	4.30	5.21	4.65	4.50	4.98	4.28	3.94	5.67	5.22	4.95	3.77
MnO	0.11	0.10	0.09	0.13	0.09	0.11	0.11	0.06	0.10	0.12	0.12	0.08	0.10
MgO	3.35	2.44	2.30	2.56	2.48	2.52	2.68	2.30	2.67	2.50	2.73	2.62	1.68
CaO	4.25	3.06	3.30	2.73	3.43	2.98	3.87	3.35	2.85	3.42	3.27	2.91	2.96
Na_2O	3.74	4.05	4.22	4.29	4.11	4.05	4.33	4.53	3.82	4.46	4.39	4.59	4.14
K_2O	5.03	5.26	5.18	5.52	4.99	5.41	4.79	5.80	5.62	5.33	5.42	5.50	6.14
P_2O_5	0.32	0.30	0.29	0.34	0.30	0.33	0.33	0.36	0.29	0.37	0.34	0.31	0.27
LOI	1.82	4.71	0.25	0.59	0.64	3.41	0.39	0.74	5.80	0.73	0.30	1.54	1.74
ASI	0.85	0.89	0.92	0.97	0.93	0.94	0.91	0.91	0.92	1.03	0.93	0.92	0.94
Total	98.87	98.83	98.07	99.53	100.69	98.55	99.68	100.28	98.26	100.35	100.46	100.44	98.22

tFe_2O_3, total iron oxide as ferric iron; LOI, loss on ignition; nd, not determined; ASI, Aluminum Saturation Index [White & Chappell, 1988; molar (Al_2O_3)/ molar $(CaO+Na_2O+K_2O)$]; abbreviations of rock types are as follows: qsy, quartz syenite; qmz, quartz monzonite; sy, syenite; mz, monzonite.

$^{206}Pb/^{204}Pb$ ratios of analysed zircon grains should be >5000, and (2) the analysed rock samples should be sufficiently old (several 100 Ma) since the ^{207}Pb-^{206}Pb ratio in young rocks is very low and less time dependent than in older rocks. As clearly seen from Table 5, the $^{206}Pb/^{204}Pb$ ratios of the measured grains are fairly low (3125, 862, 610 and 222) and those with ratios <1000 especially can yield completely misleading age information if the common lead composition of the zircon is not correctly estimated. However, using the Stacey & Kramers (1975) method for common lead correction does not seem to provide a reliable correction unless the Pb in the Kösedağ magma is conformable with the Stacey & Kramers (1975) lead data, and this can only be known by measuring the lead composition of feldspar crystals extracted from the same rock sample from which zircon grains were separated. Unfortunately, we do not have such data yet. However, despite these two discrepancies, i.e. low ^{206}Pb-^{204}Pb ratio < 5000 and the lack of Pb composition of co-existing feldspars, the analysed zircon grains seem to yield an acceptable age for the Kösedağ pluton which can be considered to be within the error range of the only known Rb-Sr wholerock isochron of 42±4 Ma (Kalkancı 1974).

Discussion

Fractional Crystallization

The quartz syenites seem to be derived through fractional crystallization (FC). They are mainly exposed within the central part of the pluton. Increasing quartz contents in the quartz syenites in modal mineralogy and of silica

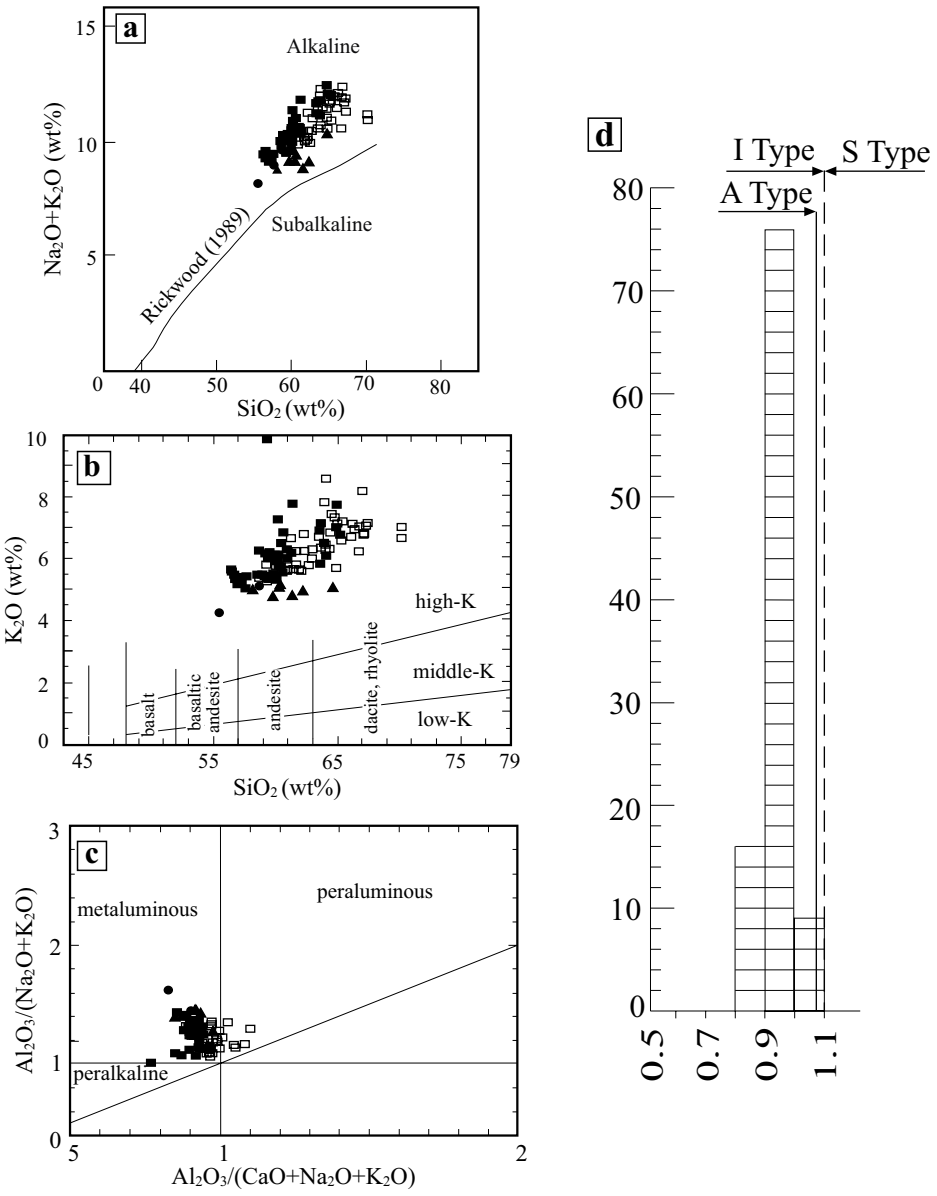

Figure 4. Major element geochemical discrimination diagrams of the Kösedağ syenitic pluton. **(a)** Total alkalis vs silica (after Irvine & Baragar 1971; dividing line between alkaline and subalkaline fields after Rickwood 1989); **(b)** K_2O vs silica (after Le Maitre *et al.* 1989); and **(c)** Shand index; **(d)** frequency distribution of ASI (Aluminum Saturation Index= molar Al_2O_3/molar ($CaO+Na_2O+K_2O$); White & Chappell 1988). Symbols are as in Figure 3.

content in whole-rock geochemical composition is consistent with a FC process that modified the composition of magma during crystallization. Decrease of Al_2O_3, tFe_2O_3, MgO, CaO, TiO_2, MnO, P_2O_5 and increase of Na_2O and K_2O contents with increasing silica is particularly considered to be evidence of FC. Furthermore, the negative Eu anomaly, seen only in the quartz syenites, is considered to indicate plagioclase fractionation in the first FC product, i.e. in the syenites during the crystallization of magma source of Kösedağ syenitic pluton.

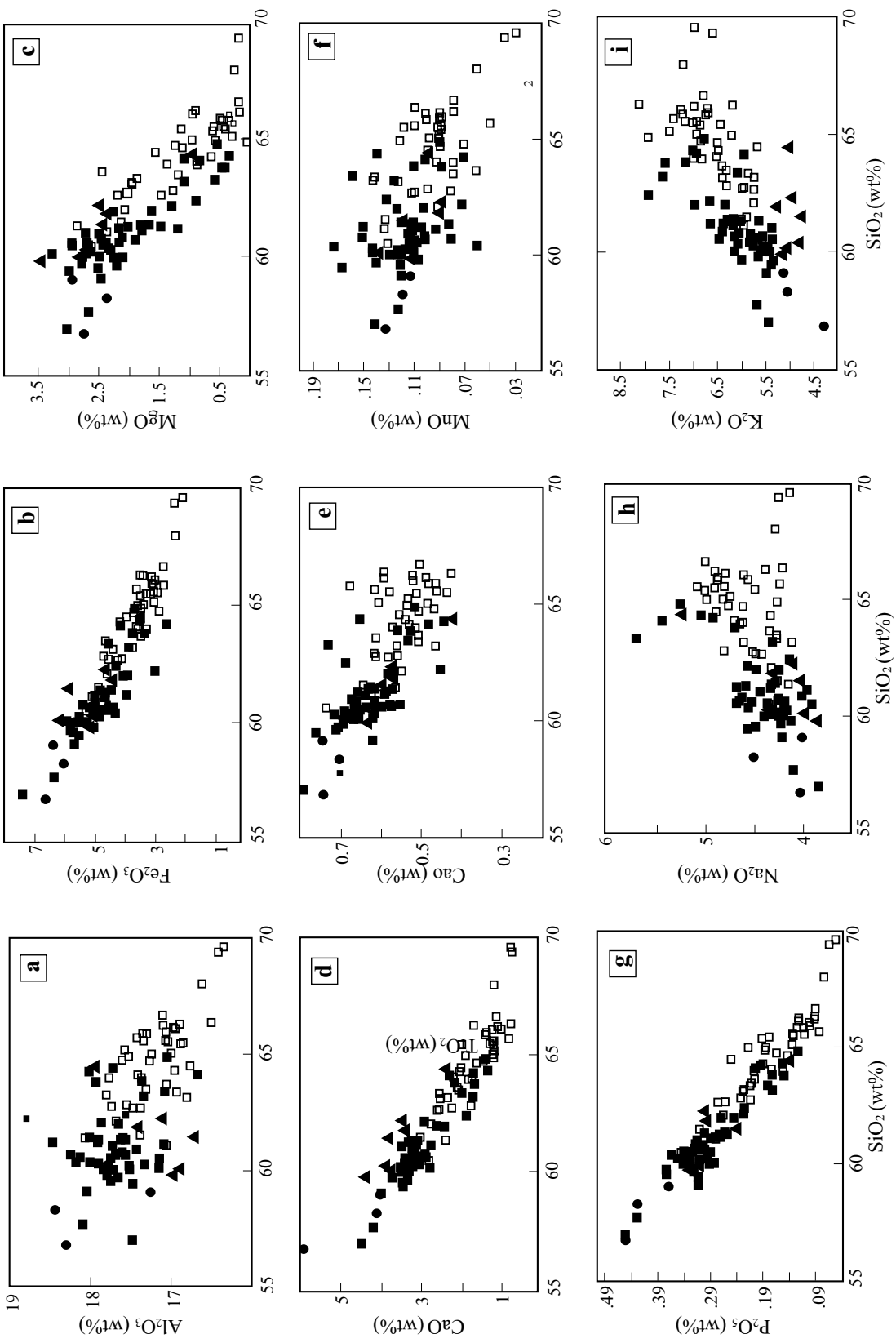

Figure 5. Major element oxides vs silica variograms of the Kösedağ syenitic pluton (see text for explanation). Symbols are as in Figure 3.

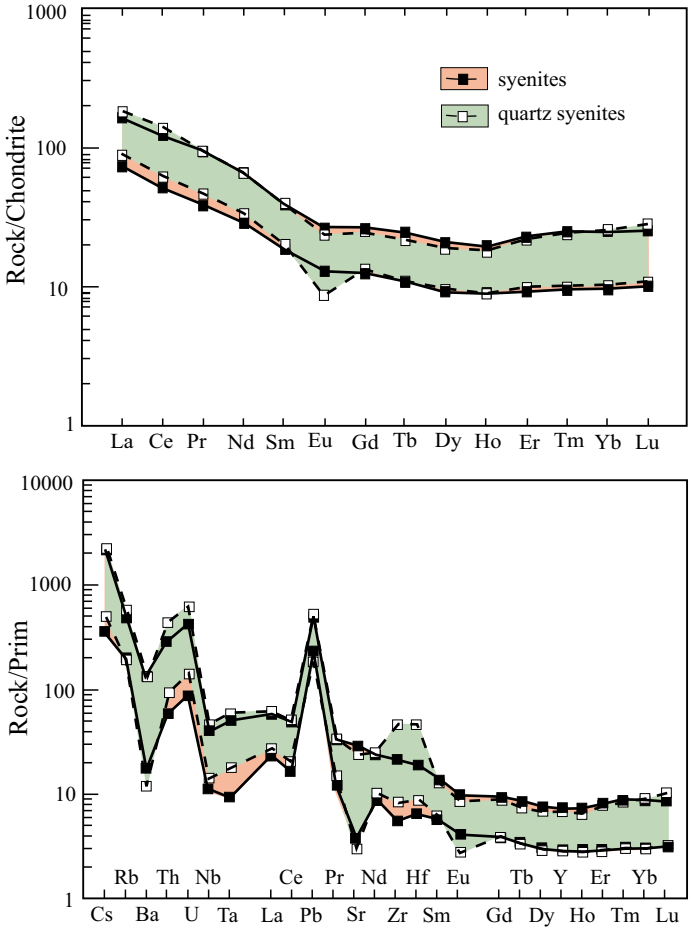

Figure 6. Chondrite-normalized REE and Prim (primordial mantle)-normalized spider diagrams of the Kösedağ syenitic pluton. Normalization values after Sun & McDonough (1989). Symbols are as in Figure 3.

Source Characteristics

All the samples from the Kösedağ syenitic pluton plot either in or next to the arc volcanics subfield in the Ce/Pb vs Ce and Nb/Th vs Nb diagrams (Figure 8a, b). Such an arc-like geochemical composition seems to be sourced either from subduction zone enrichment or crustal contamination in the Rb/Y vs Nb/Y plot (Pearce *et al.* 1990) (Figure 8c). The Th/Yb vs Ta/Yb plot, which is a commonly used HFSE ratio/ratio diagram in igneous petrogenesis (e.g., Pearce 1982; Pearce *et al.* 1990), reveals a FC (fractional crystallization)-related genesis, although the first crystallized rocks plot next to the subduction zone metasomatism subfield (Figure 8d). The Ba/Nb vs La/Nb (Jahn *et al.* 1999) plot indicates a multi-sourced material involvement in the genesis of the

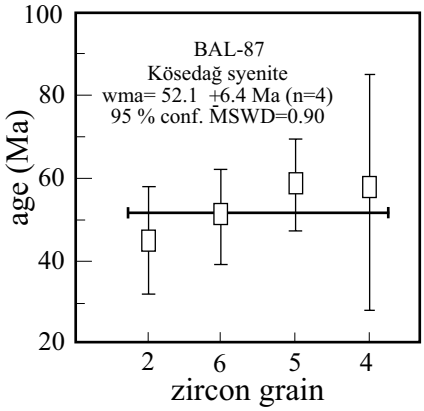

Figure 7. Weighted-mean ages (WMA) of zircon grains extracted from the Kösedağ syenitic pluton. MSWD= mean squares of weighted deviates (see Figure 2 and Table 5 for location and other explanations).

Table 4. Whole-rock trace and REE composition (ppm) of selected samples from the Kösedağ syenitic pluton.

Sample	BAL85	BAL86	BAL87	BAL88	BAL89	BAL90	BAL91	BAL92	BAL93	BAL94	BAL95	BAL96	BAL97	BAL98	BAL99
Rock type	qsy	qsy	qsy	qsy	qsy	qsy	qsy	qsy	qsy	qsy	qsy	sy	sy	sy	sy
Mo	6	7	7	6	3	5	7	6	5	4	8	7	7	6	6
Cu	18	27	15	43	36	70	49	70	61	71	62	22	20	107	35
Pb	26	23	26	31	15	26	37	29	33	32	27	34	24	18	26
Zn	nd	47	39	71	nd	31	49	53	45	62	48	63	58	72	39
As	9	15	18	32	11	11	17	9	17	23	nd	15	nd	nd	5
Sb	1.0	1.6	2.7	2.8	1.7	2.0	2.4	2.4	1.6	3.3	1.1	2.2	0.5	0.9	0.5
Bi	0.8	nd	0.8	1.6	0.4	0.6	1.2	0.7	1.2	1.7	0.7	0.7	nd	1.0	0.8
Tl	0.6	0.5	0.8	0.6	0.6	0.8	1.1	0.5	0.6	0.4	0.4	0.7	0.4	0.2	0.4
Co	2	7	2	4	5	6	7	8	7	9	8	3	4	12	5
Cr	nd	nd	nd	nd	nd	nd	199	nd	nd	nd	26	nd	nd	nd	21
V	15	69	13	37	38	61	63	82	82	103	96	26	80	128	66
Ba	110	908	87	444	347	583	660	678	743	725	621	124	774	775	837
Cs	8.0	11.4	16.1	18.5	4.3	9.5	7.1	7.3	6.8	5.2	6.6	16.0	4.6	2.9	4.4
Ga	16	16	17	15	9	16	17	16	17	18	17	18	16	16	17
Hf	6.5	6.0	13.4	8.3	4.6	6.5	7.7	10.1	5.1	5.6	3.1	4.0	2.2	3.5	5.6
Nb	17	17	32	22	11	19	25	16	16	18	12	26	11	10	8
Rb	297	197	362	248	124	200	239	214	214	207	179	309	212	131	179
Sn	2	2	4	3	1	2	2	2	2	3	2	4	2	1	1
Sr	72	495	66	247	230	395	371	455	502	515	446	84	307	560	540
Ta	1.2	1.3	2.3	1.9	0.8	1.3	1.7	1.0	1.0	1.1	0.8	2.0	0.7	0.6	0.4
Th	17.9	24.8	36.8	29.6	13.8	22.8	24.1	16.3	14.7	18.3	8.6	24.2	9.6	6.9	5.3
U	4.8	10.5	11.6	12.8	3.3	8.0	7.9	5.1	3.7	7.0	3.5	8.8	2.9	2.5	2.1
W	3	4	3	5	2	3	5	3	3	3	3	3	2	1	2
Zr	248	200	494	269	151	217	266	391	178	207	103	96	66	121	232
Y	23	25	30	25	14	24	27	25	20	26	20	32	14	21	17
La	36.2	34.6	42.1	32.0	20.7	37.1	40.2	30.8	29.7	33.9	30.0	38.5	17.2	27.9	23.8
Ce	66.3	66.5	84.6	65.0	37.5	69.9	76.5	57.4	55.4	63.9	55.7	74.9	31.3	53.4	42.8
Pr	7.37	7.76	9.04	7.14	4.40	7.94	8.74	6.81	6.47	7.75	6.55	8.79	3.60	6.62	5.10
Nd	24.7	27.4	29.2	24.4	15.5	27.5	30.4	24.5	23.4	27.9	24.1	30.3	13.2	25.3	18.7
Sm	4.7	5.6	5.6	4.8	3.0	5.2	5.9	4.8	4.5	5.6	4.9	5.9	2.8	5.2	3.8
Eu	0.59	1.31	0.50	0.83	0.66	1.05	1.13	1.24	1.30	1.31	1.36	0.74	1.34	1.52	1.32
Gd	4.1	5.0	4.7	4.1	2.7	4.5	5.1	4.4	4.2	5.1	4.2	5.3	2.5	4.6	3.3
Tb	0.7	0.8	0.8	0.8	0.4	0.8	0.8	0.7	0.7	0.8	0.7	0.9	0.4	0.7	0.5
Dy	3.7	4.4	4.7	4.2	2.4	4.0	4.5	4.0	3.6	4.2	3.5	5.2	2.3	3.7	2.9
Ho	0.8	0.9	1.0	0.9	0.5	0.8	0.9	0.9	0.7	0.9	0.7	1.1	0.5	0.8	0.6
Er	2.7	2.9	3.6	3.1	1.6	2.7	3.1	2.7	2.3	2.8	2.3	3.7	1.5	2.3	1.9
Tm	0.44	0.46	0.61	0.50	0.25	0.43	0.49	0.43	0.37	0.43	0.34	0.63	0.24	0.35	0.28
Yb	2.9	3.1	4.3	3.6	1.7	2.9	3.3	2.9	2.4	2.8	2.2	4.2	1.6	2.2	1.9
Lu	0.48	0.50	0.72	0.59	0.27	0.46	0.54	0.49	0.38	0.44	0.36	0.64	0.25	0.35	0.29
Eu/Eu*	0.41	0.76	0.30	0.57	0.71	0.66	0.63	0.82	0.91	0.75	0.92	0.41	1.55	0.95	1.14
$(La/Yb)_{CN}$	8.95	8.00	7.02	6.38	8.73	9.18	8.74	7.62	8.88	8.69	9.78	6.57	7.71	9.10	8.98

See Table 3 for explanation of rock type; Eu/Eu* [= $Eu_{CN}/(Sm_{CN} \cdot Gd_{CN})^{0.5}$]; chondrite normalizing values were taken after Sun & McDonough (1989); nd, not determined.

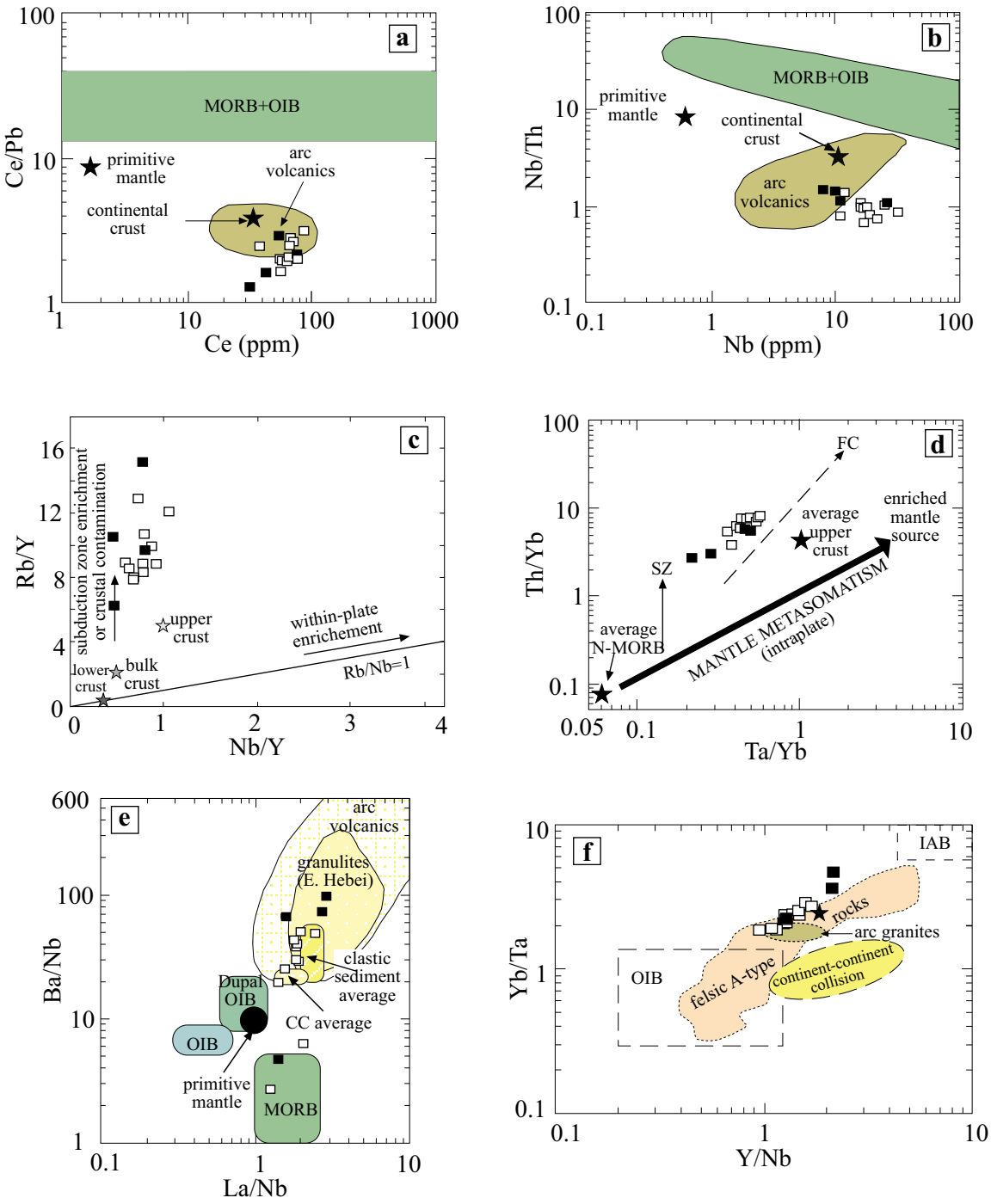

Figure 8. (a) Ce/Pb vs Ce, (b) Nb/Th vs Nb, (c) Rb/Y vs Nb/Y, (d) Th/Yb vs Ta/Yb (Pearce *et al.* 1990), (e) Ba/Nb vs La/Nb (Jahn *et al.* 1999) and (f) Yb/Ta vs Y/Nb (Best & Christiansen 2001) plots of the Kösedağ syenitic pluton. Primitive mantle after Hofmann (1988); continental crust, MORB (mid-ocean ridge basalts), OIB (ocean-island basalts) and arc volcanics compositions after Schmidberger & Hegner (1999) in (a) and (b). Compositions of the lower-, bulk-, and upper crusts after Taylor & McLennan (1985); the vectors for the subduction zone enrichment or crustal contamination and within-plate enrichment are based on the data of Pearce *et al.* (1990) in (c). The vectors of SZ and FC stand for the possible subduction zone and fractional crystallization, respectively, in (d). IAB and OIB refer the island arc and oceanic island basalts, respectively, in (f). Symbols are as in Figure 3.

Kösedağ syenitic pluton, such as MORB-like mantle, mafic lower crust as reflected by the composition of granulites of Eastern Hebei, arc volcanics and clastic continental sediments (Figure 8e). The Yb/Ta vs Y/Nb variation diagram (Best & Christiansen 2001) shows that most of the rock samples from the Kösedağ pluton plot in the felsic A-type granite subfield, although some samples also reveal an arc-related signature (Figure 8f). The felsic A-type granites were considered as mantle-derived by Eby (1990, 1992).

In the light of all these geochemical characteristics, one can conclude that the material of the Kösedağ syenitic pluton was derived from a mantle source, which was metasomatized by earlier subduction-derived fluids that carry the subduction signature in the geochemical composition. This mantle source also seems to be probably lithospheric, because it has La/Nb ratios exceeding 1.0 (DePaolo & Daley 2000) (Figure 8e). The magma derived from partial melting of such a metasomatized lithospheric mantle source can also be contaminated by crustal material during ascent through the crust that shows as crustal contamination in the geochemical composition. Furthermore, FC seems to have played an important role during the crystallization of this magmatic melt, in order to yield the Kösedağ syenitic pluton.

Geodynamic Interpretation

Geotectonic discrimination diagrams of Batchelor & Bowden (1985) and Pearce *et al.* (1984) reveal a late orogenic (Figure 9a) and post-collisional setting with a subduction-related signature for the Kösedağ syenitic pluton (Figure 9b, c), respectively. The regional geological and tectonic setting confirms that the Kösedağ syenitic pluton was emplaced in a post-collisional extension-related geodynamic regime, following the continent-continent collision between the Eurasian plate (EP) and Tauride-Anatolide platform (TAP) along the İzmir-Ankara-Erzincan (IAE) suture zone (Figure 10a) (Şengör & Yılmaz 1981; Yılmaz *et al.* 1997; Okay & Şahintürk 1997). The apatite fission-track geothermochronology study of Boztuğ *et al.* (2004) performed on the granitoid rocks in the east-central Pontides, cropping out between Dereli in the north and Şebinkarahisar in the south, reveals that rapid tectonic uplift occurred in the time interval between ca. 57 and 47 Ma. This fast tectonic uplift was attributed, by Boztuğ *et al.* (2004), to the continent-continent collision between the EP and TAP in the east-central Pontides.

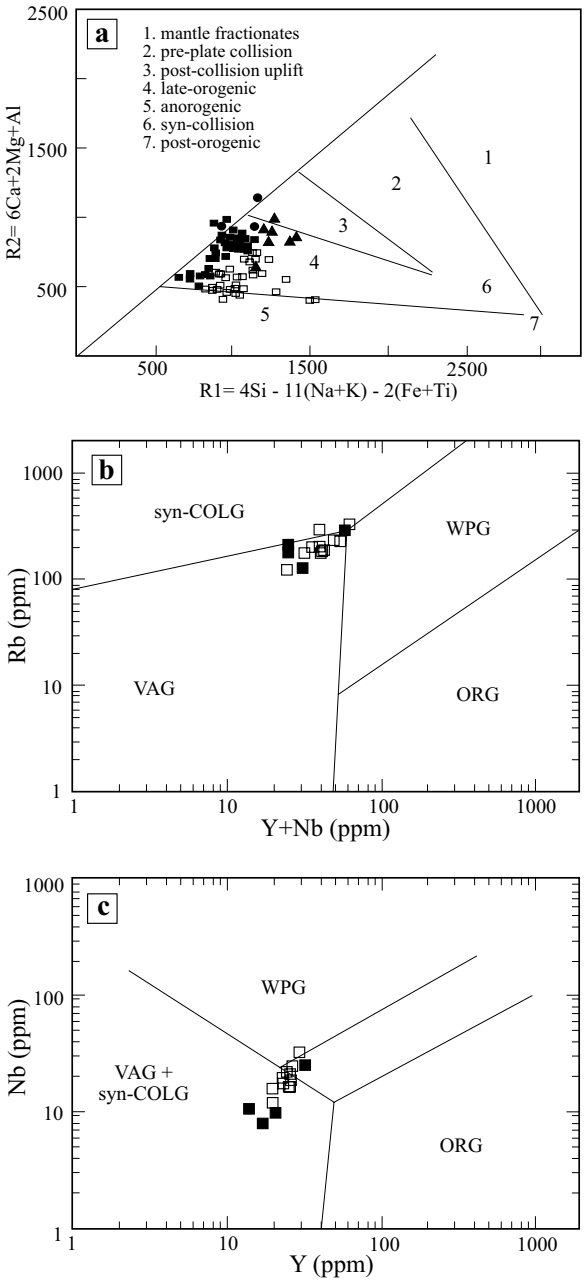

Figure 9. (a) R1 vs R2 (Batchelor & Bowden 1985), (b) Rb (ppm) vs Y+Nb (ppm) and (c) Nb (ppm) vs Y (ppm) (Pearce *et al.* 1984) geotectonic discrimination diagrams for the Kösedağ syenitic pluton. Syn-COLG– syn-collisional granitoids; WPG– within-plate granitoids; VAG– volcanic-arc granitoids; ORG– ocean-ridge granitoids. Symbols are as in Figure 3.

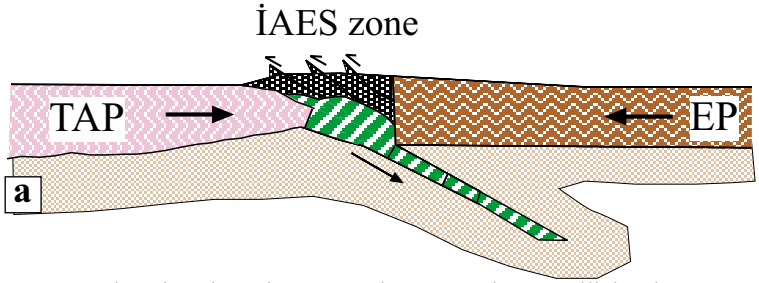

compressional regime due to continent-continent collision between TAP and EP along the IAE suture zone leading to rapid uplift of basement rocks including the central Anatolian granitoids (ca. 62-57 Ma)

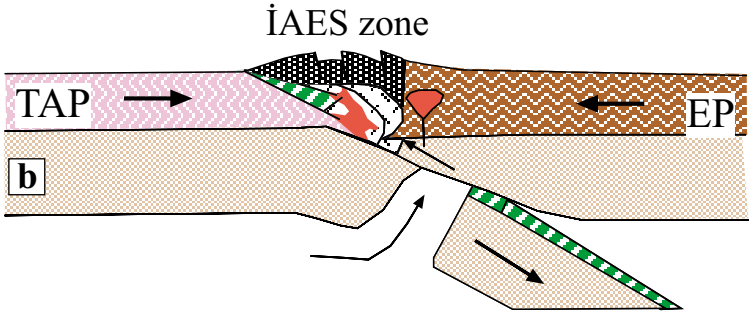

upwelling and advection of hot asthenosphere into the base of lithosphere, emplacement of slab break-off-related multi-sourced granitoids, and tectonic uplift of basement rocks including pre-Eocene granitoids in the east-central Pontide region (ca. 55-45 Ma)

Figure 10. (a) Suggested geodynamic model for the continent-continent collision between the Tauride-Anatolide platform (TAP) and the Eurasian plate (EP) along the İzmir-Ankara-Erzincan suture zone (IAESZ) (after Boztuğ & Jonckheere 2007), and (b) slab break-off driven regional extensional geodynamic setting following the continent-continent collision.

Table 5. ^{207}Pb / ^{206}Pb single-zircon evaporation data.

Sample-zircon No	Geographic coordinates	Numb. of scans	^{207}Pb / ^{206}Pb	^{204}Pb / ^{206}Pb	^{207}Pb / $^{206}Pb_{corr}$	^{207}Pb / ^{206}Pb Age (Ma ± 2 sigma error)
BAL87-Z2	40°05′10.04″N					
	37°58′08.20″E	90	0.051414±(164)	0.00032±(011)	0.046916±(152)	44.9±12.9
BAL87-Z6		90	0.063746±(124)	0.00116±(012)	0.047027±(118)	50.5±11.2
BAL87-Z5		90	0.070822±(340)	0.00164±(026)	0.047179±(114)	58.3±11.0
BAL87-Z4		79	0.11256±(300)	0.0045±(212)	0.047145±(458)	56.5±28.4
Weighted Mean Age						52.1±6.4

Uncertainties for the ^{207}Pb / ^{206}Pb, ^{204}Pb / ^{206}Pb and ^{207}Pb / $^{206}Pb_{corr}$ ratios are 2 sigma errors in the last three digits (in parantheses).

The time-space relationships between the multi-sourced Eocene granitoids exposed across the entire eastern Pontides and fast tectonic uplift of the Dereli-Şebinkarahisar region granitoids may suggest a slab break-off-induced regional extensional tectonic regime, as recently reported by Boztuğ *et al.* (2005a) (Figure 10b). Such an extensional regime, caused by buoyancy-driven detachment (Davies & von Blanckenburg 1995; von Blanckenburg & Davies 1995) of the subducted denser oceanic lithosphere from the lighter continental lithosphere which followed it during continental collision between the EP and TAP, seems also to be spatially and temporally consistent with the opening of fault-controlled Eocene volcano-sedimentary basins throughout the eastern Pontides. The advection of hot asthenosphere to the base of the continental lithosphere induced partial melting of enriched metasomatic layers (already chemically modified by the preceding subduction-derived fluids), which were already accreted into the collision zone as tectonic slices, producing both the high-K alkaline magmas of the Kösedağ syenitic pluton in the east-central Pontides and calc-alkaline magmas of the other Eocene granitoids across the Pontides. The detachment and subsequent rebound of the continental lithosphere from the down-pulling oceanic lithosphere may have triggered fast tectonic denudation of the Dereli-Şebinkarahisar region granitoids and opened fault-controlled Eocene volcano-sedimentary basins in the eastern Pontide region (Figure 10b).

Conclusions

The Kösedağ pluton intrudes the Eocene volcano-sedimentary sequence and is unconformably covered by Lower Miocene (Aquitanian) lagoonal limestones. The main rock types are syenites and quartz syenites with a phaneritic-porphyritic texture characterized by K-feldspar megacrysts. Major element geochemical composition reveals a high-K, alkaline, metaluminous to slightly peraluminous characteristics with a low ASI value. Chondrite-normalized REE distribution patterns show upward-concave shapes without significant fractionation between LREE and HREE. Only the quartz syenites have a negative Eu anomaly, which results from plagioclase fractionation. Fractional crystallization seems to be the major process which modified the composition of the magma source of the Kösedağ syenitic pluton, forming first the syenites and then the quartz syenites. Trace element geochemistry data reveal a mantle source which was metasomatized by subduction-derived fluids with a recognizable geochemical arc-related signature. These metasomatized mantle layers were accreted into the collision zone as tectonic slices, and their subsequent partial melting could have produced the magma source of the Kösedağ syenitic pluton. Spatial and temporal relations between the Kösedağ syenitic pluton and the regional tectonic setting reveal that this partial melting could have occurred in an extension-related geodynamic setting induced by slab break-off following Late Paleocene to Early Eocene continent-continent collision between the Eurasian plate and Tauride-Anatolide platform along İzmir-Ankara-Erzincan suture zone.

Acknowledgements

This paper is part of a project supported by TÜBİTAK-Ankara (YDABÇAG-9) and CUBAP of Cumhuriyet University (M-255), Sivas, Turkey. The author is indebted to TÜBİTAK for a TÜBİTAK-BAYG grant, to DFG for a TÜBİTAK-DFG grant, and to DAAD for a grant to do research in the laboratories of the Mineralogical Institutes of the TU Bergakademie Freiberg, Germany. Dr. Marion Tichomirowa and Mr. Klaus Bombach are kindly thanked for the ^{207}Pb-^{206}Pb single zircon evaporation age determination. Prof. M. Satır and Prof. W. Siebel (Tübingen University, Germany) and Prof. Y.K. Kadıoğlu (Ankara University, Turkey) are kindly thanked for their helpful comments which improved the manuscript. I am especially indebted to Prof. Satır and Prof. Siebel for their corrections on the single zircon ^{207}Pb-^{206}Pb evaporation age section of the manuscript. Prof. J. Winchester (University of Keele, England) and Prof. E. Bozkurt (METU, Ankara, Turkey) are kindly thanked for their correction of English and editorial handling.

References

AKINCI, Ö.T. 1985. The Eastern Pontide volcano-sedimentary belt and associated massive sulphide deposits. *In*: DIXON, J.E. & ROBERTSON, A.H.F. (eds), *The Geological Evolution of the Eastern Mediterranean*. Geological Society, London, Special Publications **17**, 415–428.

ARSLAN, M. & ASLAN, Z. 2006. Mineralogy, petrography and whole-rock geochemistry of the Tertiary granitic intrusions in the Eastern Pontides, Turkey. *Journal of Asian Earth Sciences* **27**, 177–193.

BARKA, A.A. 1992. The North Anatolian fault zone. *Annales Tectonicae* **6**, 164–195.

BATCHELOR, B. & BOWDEN, P. 1985. Petrogenetic interpretation of granitoid rock series using multicationic parameters. *Chemical Geology* **48**, 43–55.

BEST, M. & CHRISTIANSEN, E.H. 2001. *Igneous Petrology*. Blackwell Science, Ann Arbor.

BİNGÖL, E. 1989. *1:2.000.000 Scale Geological Map of Turkey*. Mineral Research and Exploration Institute (MTA) of Turkey Publications, Ankara.

BOZKURT, E. 2001. Neotectonics of Turkey–a synthesis. *Geodinamica Acta* **14**, 3–30.

BOZKURT, E. & MITTWEDE, S.K. 2001. Introduction to the geology of Turkey – a synthesis. *International Geology Review* **43**, 578–594.

BOZTUĞ, D. 2001. *Suşehri (Sivas) — Gölköy (Ordu) Arasında KAFZ'nun Kuzey ve Güney Kesimlerindeki Granitoyidlerin ve Çevre Kayaçlarının Petrolojik İncelenmesi [Petrology of Granitoid and Their Country Rocks Exposed in the Northern and Southern Blocks of the NAFZ in the Area Between Suşehri (Sivas) and Gölköy (Ordu)]*. TÜBİTAK Project Report no: 195Y001-YDABÇAG-9 Sivas [in Turkish with English Abstract, unpublished].

BOZTUĞ, D., ERÇİN, A.İ., KURUÇELİK, M.K., GÖÇ, D., KÖMÜR, İ. & İSKENDEROĞLU, A. 2006. Geochemical characteristics of the composite Kaçkar batholith generated in a Neo-Tethyan convergence system, eastern Pontides, Turkey. *Journal of Asian Earth Sciences* **27**, 286–302.

BOZTUĞ, D. & HARLAVAN, Y. 2007. K-Ar ages of granitoids unravel the stages of Neo-Tethyan convergence in the eastern Pontides and central Anatolia, Turkey. *International Journal of Earth Sciences* [doi:10.1007/s00531-007-0176-0].

BOZTUĞ, D. & JONCKHEERE, R.C. 2007. Apatite fission-track data from central-Anatolian granitoids (Turkey): constraints on Neo-Tethyan closure. *Tectonics* **26**, TC3011, doi:10.1029/ 2006TC001988.

BOZTUĞ, D., JONCKHEERE, R.C., ARSLAN, M., ŞEN, C., KARSLI, O., & ERÇİN, A.İ. 2005a. Eocene slab break-off revealed by the E–W distribution of the multi-sourced granitoids and tectonic denudation in the eastern Pontides, Turkey. *Geophysical Research Abstracts, Vol. 7, 02129, 2005. SRef-ID: 1607-7962/gra/ EGU05-A-02129.*

BOZTUĞ, D., JONCKHEERE, R.C., ENKELMANN, E., RATSCHBACHER, L. & WAGNER, G.A. 2005b. Geodynamic implications of rapid denudation of the granitoids at about 50 and 20 Ma in the eastern Pontides, Turkey: apatite fission-track results. G*eochimica et Cosmochimica Acta, 69, 10, Supplement 1, Goldschmidt Conference Abstract, 2005, Geochronology of Tectonic Processes, A 300.*

BOZTUĞ, D., JONCKHEERE, R., WAGNER, G.A. & YEĞİNGİL, Z. 2004. Slow Senonian and fast Paleocene–early Eocene uplift of the granitoids in the central eastern Pontides, Turkey: apatite fission-track results. *Tectonophysics* **382**, 213–228.

BOZTUĞ, D., JONCKHEERE, R.C., WAGNER, G.A., ERÇİN, A.İ. & YEĞİNGİL, Z. 2007. Titanite and zircon fission-track dating resolves successive igneous episodes in the formation of the composite Kaçkar batholith in the Turkish Eastern Pontides. *International Journal of Earth Sciences* **96**, 875–886.

BOZTUĞ, D., KUŞÇU, İ., ERÇİN, A.İ. & AVCI, N. 2003. Mineral deposits associated with the pre-, syn- and post-collisional granitoids of the Neo-Tethyan convergence system between the Eurasian and Anatolian plates in NE and Central Turkey. *In*: ELIOPOULOS, D.G. *et al.* (eds), *Mineral Exploration and Sustainable Development*. Millpress, Rotterdam, 1141–1144.

BOZTUĞ, D., YILMAZ, S. & KESGİN, Y. 1994. İç-Doğu Anadolu alkalin provensindeki Kösedağ plütonu (Suşehri-KD Sivas) doğu kesiminin petrografisi, petrokimyası ve petrojenezi [Petrography, petrochemistry and petrogenesis of the eastern part of Kösedağ pluton from the Central-Eastern Anatolian alkaline province, Suşehri, NE Sivas]. *Türkiye Jeoloji Bülteni* **37**, 1–14 [in Turkish with English abstract].

CHAPPELL, B.W. & WHITE, A.J.R. 1974. Two contrasting granite types. *Pacific Geology* **8**, 173–174.

CLARKE, A.B. 1992. *Granitoid Rocks*. Chapman & Hall, London.

DAVIES, J.H. & VON BLANCKENBURG, F. 1995. Slab breakoff: a model of lithosphere detachment and its test in the magmatism and deformation of collisional orogens. *Earth and Planetary Science Letters* **129**, 85–102.

DEBON, F. & LE FORT, P. 1983. A chemical-mineralogical classification of common plutonic rocks and associations. *Transactions of the Royal Society of Edinburgh: Earth Sciences* **73**, 135–149.

DELALOYE, M., ÇOĞULU, E. & CHESSEX, R. 1972. Etude géochronometrique des massifs cristallins de Rize et de Gümüşhane, Pontides Orientales (Turquie). *Archives des Sciences Physiques et Naturelles* 25, Supplement **7**, 43–52.

DEPAOLO, D.J. & DALEY, E.E. 2000. Neodymium isotopes in basalts of the southwest basin and range and lithospheric thinning during continental extension. *Chemical Geology* **169**, 157–185.

EBY, G.N. 1990. The A-type granitoids: a review of their occurrence and chemical characteristics and speculation on their petrogenesis. *Lithos* **26**, 115–134.

EBY, G.N. 1992. Chemical subdivision of the A-type granitoids: petrogenetic and tectonic implications. *Geology* **20**, 641–644.

GOVINDARAJU, K. 1989. 1989 Compilation of working values and sample description for 272 geostandards. *Geostandards Newsletter* **13**, 1–113.

HEMPTON, M.R. 1987. Constraints on Arabian plate motion and extensional history of the Red Sea. *Tectonics* **6**, 687–705.

HOFMANN, A.W. 1988. Chemical differentiation of the Earth. The relationship between mantle, continental crust and oceanic crust. *Earth and Planetary Science Letters* **90**, 297–314.

HUBERT-FERRARI, A., ARMIJO, R., KING, G., MEYER, B. & BARKA, A. 2002. Morphology, displacement, and slip rates along the North Anatolian Fault, Turkey. *Journal of Geophysical Research* **107**(B10), Art. No. 2235.

IRVINE, T.N. & BARAGAR, W.R.A. 1971. A guide to the chemical classification of common volcanic rocks. *Canadian Journal of Earth Sciences* **8**, 523–548.

JAHN, B.M., WU, F., LO, C-H. & TSAI, C-H. 1999. Crust-mantle interaction induced by deep subduction of the continental crust: geochemical and Sr-Nd isotopic evidence from post-collisional mafic-ultramafic intrusions of the northern Dabie complex, central China. *Chemical Geology* **157**, 119–146.

JICA 1986. *The Republic of Turkey Report on the Cooperative Mineral Exploration of Gümüşhane Area, Consolidated Report*. Japanese International Cooperation Agency, Metal Mining Agency of Japan.

KALKANCI, Ş. 1974. *Etude géologique et pétrochimique du sud de la region de Suşehri: Géochronologie du massif syenitique de Kösedağ (NE de Sivas-Turquie)*. These de doctorat de 3eme cycle, L'Universite de Grenoble.

KARSLI, O., AYDIN, F. & SADIKLAR, M.B. 2002. Geothermobarometric investigation of the Zigana Granitoid, eastern Pontides, Turkey. *International Geology Review* **44**, 277–286.

KARSLI, O., AYDIN, F., SADIKLAR, M.B., ALTHERR, R. & UYSAL, I. 2004a. Higher degrees hybridisation in Eocene aged granitoid rocks, NE Turkey: as indicator of oxygen fugacity from mafic microgranular enclaves and host rocks. *Proceedings of the 5th International Symposium on Eastern Mediterranean Geology,* Thessaloniki, Greece, 14–20 April, 2004, Ref. T2–41

KARSLI, O., AYDIN, F. & SADIKLAR, M.B. 2004b. Magma interaction recorded in plagioclase zoning in granitoid systems, Zigana Granitoid, Eastern Pontides, Turkey. *Turkish Journal of Earth Sciences* **13**, 287–305.

KARSLI, O., CHEN, B., AYDIN, F. & ŞEN, C. 2007. Geochemical and Sr-Nd-Pb isotopic compositions of the Eocene Dölek and Sarıçiçek plutons, eastern Turkey: implications for magma interaction in the genesis of high-K calc-alkaline granitoids in a post-collision extensional setting. *Lithos* **98**, 67–96.

KAYGUSUZ, A., SIEBEL, W., ŞEN, C. & SATIR, M. 2007. Petrochemistry and petrology of I-type granitoids in an arc setting: composite Torul pluton, Eastern Pontides, NE Turkey. *International Journal of Earth Sciences* (doi:10.1007/s00531-007-0188-9).

KAZMIN, V.G., SCHREIDER, A.A. & BULYCHEV, A.A. 2000. Early stages of evolution of the Black Sea. *In*: BOZKURT, E., WINCHESTER, J.A. & PIPER, J.D.A. (eds), *Tectonics and Magmatism in Turkey and the Surrounding Area*. Geological Society, London, Special Publications **173**, 235–249.

KOBER, B. 1986. Whole-grain evaporation for Pb^{207}/Pb^{206} age investigations on single zircons using a double-filament thermal ion-source. *Contributions to Mineralogy and Petrology* **93**, 482–490.

KOBER, B. 1987. Single zircon evaporation combined with Pb emitter bedding for Pb^{207}/Pb^{206} age investigations using thermal ion mass spectrometry, and implications to zirconology. *Contributions to Mineralogy and Petrology* **96**, 63–71.

LE MAITRE, R,W., BATEMAN, P., DUDEK, A., KELLER, J., LAMEYRE, J., LE BAS, M.J., SABINE, P.A., SCHMID, R., SORENSEN, H., STRECKEISEN, A., WOOLLEY, A.R. & ZANETTIN, B. 1989. *A Classification of Igneous Rocks and Glossary of Terms: Recommendations of the International Union of Geological Sciences Subcommission on the Systematics of Igneous Rocks*. Blackwell Science Publication.

LE PICHON, X., CHAMOT-ROOKE, N., LALLEMANT, S., NOOMEN, R. & VEIS, G. 1995. Geodetic determination of the kinematics of central Greece with respect to Europe: implications for eastern Mediterranean tectonics. *Journal of Geophysical Research* **B100**, 12675–12690.

MANETTI, P.Y., PECCERILLO, A., POLI, C. & CORSINI, F. 1983. Petrochemical constraints on models of Cretaceous–Eocene tectonic evolution of the Eastern Pontide chain (Turkey). *Cretaceous Research* **4**, 159–172.

OKAY, A.İ & ŞAHİNTÜRK, Ö. 1997. Geology of the Eastern Pontides. *In*: ROBINSON, A.G. (ed), *Regional and Petroleum Geology of the Black Sea and Surrounding Region*. AAPG Memoir **68**, 291–311.

OKAY, A. İ., ŞENGÖR, A.M.C. & GÖRÜR, N. 1994. Kinematic history of the opening of the Black Sea and its effect on the surrounding regions. *Geology* **22**, 267–270.

PEARCE, J.A. 1982. Trace element characteristics of lavas from destructive plate boundaries. *In*: THORPE, R.S. (ed), *Andesites*. Wiley, New York, 525–548.

PEARCE, J.A., HARRIS, N.B.W. & TINDLE, A.G.W. 1984. Trace element discrimination diagrams for the tectonic interpretation of granitic rocks. *Journal of Petrology* **25**, 956–983.

PEARCE, J.A, BENDER, J.F., DE LONG, S.E., KIDD, W.S.F., LOW, P.J., GÜNER, Y., ŞAROĞLU, F., YILMAZ, Y., MOORBATH, S. & MITCHELL, J.G. 1990. Genesis of collision volcanism in Eastern Anatolia, Turkey. *Journal of Volcanology and Geothermal Research* **44**, 189–229.

RICKWOOD, P.C. 1989. Boundary lines within petrologic diagrams which use oxides of major and minor elements. *Lithos* **22**, 247–263.

ŞAROĞLU, F. 1988. Age and offset of the North Anatolian fault. *M.E.T.U. Journal of Pure and Applied Science* **21**, 65–79.

SCHMIDBERGER, S.S. & HEGNER, E. 1999. Geochemistry and isotope systematics of calc- alkaline volcanic rocks from the Saar-Nahe basin (SW Germany)-implications for Late-Variscan orogenic development. *Contributions to Mineralogy and Petrology* **135**, 373–385.

ŞENGÖR, A.M.C., GÖRÜR, N. & ŞAROĞLU, F. 1985. Strike-slip faulting and related basin formation in zones of tectonic escape: Turkey as a case study. *In*: BIDDLE, K.T. & CHRISTIE-BLICK, N. (eds), *Strike-Slip Deformation, Basin Formation and Sedimentation.* Society of Economic Paleontology and Mineralogy, Special Publications **37**, 227–264.

ŞENGÖR, A.M.C. & KIDD, W.S.F. 1979. The post-collisional tectonics of the Turkish-Iranian Plateau and a comparision with Tibet. *Tectonophysics* **55**, 361–376.

ŞENGÖR, A.M.C., ÖZEREN, S., GENÇ, T. & ZOR, E. 2003. East Anatolian high plateau as a mantle-supported, north-south shortened domal structure. *Geophysical Research Letters* **30** (24), 8045.

ŞENGÖR, A.M.C. & YILMAZ, Y. 1981. Tethyan evolution of Turkey: a plate tectonic approach. *Tectonophysics* **75**, 181–241.

STACEY, J.S. & KRAMERS, J.D. 1975. Approximation of terrestrial lead isotope evolution by a two-stage model. *Earth and Planetary Science Letters* **26**, 207–221.

SUN, S.S. & MCDONOUGH, W.F. 1989. Chemical and isotopic systematics of oceanic basalts: implications for mantle composition and processes. *In*: SAUNDERS, A.D. & NORRY, M.J. (eds), *Magmatism in the Ocean Basins*. Geological Society, London, Special Publications no: **42**, 313–345.

TANER, M.F. 1977. *Etude géologique et pétrographique de la region de Güneyce-İkizdere, situee au Sud de Rize (Pontides Orientales, Turquie*). PhD Thesis, Universite Geneve, [unpublished].

TAYLOR, S. R. & MCLENNAN, S. M. 1985. *The Continental Crust: Its Composition and Evolution.* Blackwell Scientific, Oxford.

TOPUZ, G. & ALTHERR, R. 2004a. Pervasive rehydration of granulites during exhumation - an example from the Pulur complex, Eastern Pontides, Turkey. *Mineralogy and Petrology* **81**, 165–185.

TOPUZ, G., ALTHERR, R., SATIR, M. & SCHWARZ, W.H. 2004b. Low-grade metamorphic rocks from the Pulur complex, NE Turkey: implications for the pre-Liassic evolution of the Eastern Pontides. *International Journal of Earth Sciences* **93**, 72–91.

TOPUZ, G., ALTHERR, R., KALT, A., SATIR, M., WERNER, O. & SCHWARZ, W.H. 2004c. Aluminous granulites from the Pulur complex, NE Turkey: a case of partial melting, efficient melt extraction and crystallisation. *Lithos* **72**, 183–207.

TOPUZ, G., ALTHERR, R., SCHWARZ, W.H., SIEBEL, W., SATIR, M. & DOKUZ, A. 2005. Post-collisional plutonism with adakite-like signatures: the Eocene Saraycık granodiorite (Eastern Pontides, Turkey). *Contributions to Mineralogy and Petrology* **150**, 441–455.

TRIFONOV, V.G., KARAKHANIAN, A.S. & KOZHURIN, A.I. 1994. Major active faults of the collision area between the Arabian and the Eurasian plates. *In*: BOLT, B.A. & AMIRBEKIAN, R. (eds), *Continental Collision Zone Earthquakes and Seismic Hazard Reduction*. Proceedings of the International Conference at Yerevan-Sevan, Armenia 56–76.

VON BLANCKENBURG, F. & DAVIES, J.H. 1995. Slab breakoff: a model for syncollisional magmatism and tectonics in the Alps. *Tectonics* **14**, 120–131.

WESTAWAY, R. 1994. Present-day kinematics of the Middle East and eastern Mediterranean. *Journal of Geophysical Research* **B99**, 12071–12090.

WHITE, A.J.R. & CHAPPELL, B.W. 1988. Some supracrustal (S-type) granites of the Lachlan Fold Belt. *Transactions of the Royal Society of Edinburgh: Earth Sciences* **79**, 169–181.

YILMAZ, Y., TÜYSÜZ, O, YİĞİTBAŞ, E, GENÇ, Ş.C. & ŞENGÖR, A.M.C. 1997. Geology and tectonic evolution of the Pontides. *In*: ROBINSON, A.G. (ed), *Regional and Petroleum Geology of the Black Sea and Surrounding Region.* AAPG Memoir **68**, 183–226.

Received 15 June 2007; revised typescript received 07 December 2007; accepted 07 December 2007